ISBN : 978-979-96595-4-5

Proceeding

The 2nd International Conference of the Indonesian Chemical Society 2013

ICICS 2013

Research in Chemistry for Better Quality of Environmental

Universitas Islam Indonesia, Yogyakarta, Indonesia
October, 22 - 23th 2013

Abdul Kahar Muzakkir, Conference Hall
Universitas Islam Indonesia (UII), Yogyakarta.
Kampus Terpadu, Jl. Kaliurang KM 14,5 Sleman, Yogyakarta.

Welcoming Address by The Organizing Committee

Assalamu'alaikum Wr. Wb.

Honorable Rector of Universitas Islam Indonesia
The distinguished invited speakers, and
All participants of the ICICS 2013

Welcome you at the 2nd International Conference of the Indonesia Chemical Society 2013 (ICICS 2013) this morning here at the Auditorium Kahar Muzakkir Universitas Islam Indonesia, Yogyakarta. The international conference is an annual conference of the Indonesian Chemical Society (Himpunan Kimia Indonesia, HKI). In the year 2013, the mandate of the organizing committee was given to the HKI Yogyakarta branch and also supported by Department of Chemistry of Universitas Negeri Yogyakarta (UNY), Department of Chemistry of Universitas Gadjah Mada (UGM), Department of Chemistry of Universitas Islam Negeri Sunan Kalijaga (UIN Suka), National Nuclear Energy Agency (BATAN Yogyakarta), and Balai Penyelidikan dan Pengembangan Kegunungapian (BPPTK Yogyakarta). For the year 2013, the honor of hosting ICICS 2013 has been given to the Department of Chemistry, Faculty of Mathematics and Natural Sciences, Universitas Islam Indonesia, Yogyakarta. This conference was also prepared to celebrate 70th anniversary of Universitas Islam Indonesia.

The conference comprises both oral and poster presentation in English and Indonesian with optional post conference publication of full papers in English in the Procedia Chemistry (Elsevier, ISSN: 1876-6196) and Proceeding Conference for Indonesian language. There are 211 papers presented orally and 34 papers presented by poster covering wide-variety subjects of chemistry. We invited 6 Indonesian invited speakers, 2 Japan invited speakers, 1 Australian invited speakers, 1 Saudi Arabia invited speakers, and 1 Malaysian Invited speakers.

We hope you will enjoy a pleasant and valuable seminar at Universitas Islam Indonesia

Wassalamu'alaikum Wr. Wb.

Riyanto, Ph.D.
Chairman

ISBN: 978-979-96595-4-5

Committees

Steering Committee

1. Head of the Indonesian Chemical Society
2. Head of the Indonesian Chemical Society Yogyakarta Branch
3. Rector of Islamic University of Indonesia
4. Rector of Gadjah Mada University
5. Rector of Yogyakarta State University
6. Rector of State Islamic University of Sunan Kalijaga
7. Head of Geological Agency of Indonesia
8. Head of National Nuclear Energy Agency of Indonesia

Reviewers:

1. Prof. Dr. Hardjono Sastrohamidjojo (UII Yogyakarta)
2. Prof. Dr. Nurfina Aznam (UNY Yogyakarta)
3. Prof. Dr. Karna Wijaya (UGM Yogyakarta)
4. Prof. Harno Dwi Pranowo (UGM Yogyakarta)
5. Prof. Drs. Sahat Simbolon, M.Sc. (BATAN Yogyakarta)
6. Dr. Muhamad A. Martoprawiro (HKI)
7. Riyanto, Ph.D. (UII Yogyakarta)
8. Dr. Is Fatimah (UII Yogyakarta)

Editors:

1. Dr. Noor Fitri (UII Yogyakarta)
2. Drs. Allwar, M.Sc., Ph.D. (UII Yogyakarta)
3. Rudy Syah Putra, Ph.D. (UII Yogyakarta)
4. Dwiarso Rubiyanto, M.Si. (UII Yogyakarta)
5. Tatang Shabur Julianto, M.Si. (UII Yogyakarta)

ISBN: 978-979-96595-4-5

CONTENT

Content		Page
Cover		i
Preface		ii
Welcoming addres by The Organizing Committee		iii
Opening Speech from the Rector of Universitas Islam Indonesia		iv
Remarks by the Chairman of the Indonesian Chemical Society (Himpunan Kimia Indonesia, HKI)		v
Committe		vi
Reviewers and Editors		vi
Content		ix
Invited Speakers		
Shaobin Wang, Stacey Indrawirawan, Yunjin Yao, Hongqi Sun	Graphene Supported Oxide Systems for Catalytic Oxidation of Organic Compounds in Aqueous Solution for Water Treatment	xii
Tatsufumi Okino	Chemistry and biology of brominated compounds from marine algae *Laurencia* spp.	xv
Heriyanto, Leenawaty Limantara	Chlorophyll and Carotenoid Prospects on Food, Health and Energy	xviii
Katsumi Kaneko	Molecular Functions of 1 nm-Scale Pore Spaces and their Application Potential to Sustainable Technologies	xxviii
Fethi Kooli	Al_{13} Intercalated and Pillared Montmorillontes from Unusual Antiperspirant Aqueous Solutions: Precursors for Porous Clay Heterostructures and Heptane Hydro-Isomerization Catalytic Activities	xxxi
Allwar, Ahmad Md. Noor, Mohd Asri bin Mohd Nawi	Characterizing Microporous Structures using Nitrogen Adsorption-Desorption Isotherm for Activated Carbon Prepared with Different Zinc Chloride Concentrations	xxxv
Papers of Analytical Chemistry		
Ariestya Arlene A., Anastasia Prima K.	Extraction Equilibrium Curve of Red Food Coloring From Rosella	1-6
Bambang Purwono, Tutik Dwi Wahyuningsih, Widya Hadi Kusmawan	Synthesis of 2-Allyl-6-Methoxy-4-Phenyliminomethyl Phenol from Vanillin and Its Used as An Acid-Base Titration Indicator	7-12
Barlah Rumhayati, Chasan Bisri, Risma Putri Disicahyani	Removal of Heavy Metals and Nutrients in Drinking Water Sources using Acrylamide Hydrogel Pairs Containing Ferrihydrite and Chelex-100 Adsorbents	13-19
Budiana I Gusti M. Ngurah, Jumina, Chairil Anwar, Mustofa	Synthesis and Characterization of Benzoyl octaethoxycalix[4]arene for UV Radiation Protection	20-27
Deswati, Hamzar Suyani, Hilfi Pardi and Umiati Loekman	The Method of the Development Analysis of Fe, Co, Ni and Cr by Adsorptive Stripping Voltammetry (AdSV) for Monographs the Determination of Trace Metals	28-36

Eva Maria Widyasari, Iswahyudi	Abnormal Toxicity Test on Radiopharmaceutical ^{99m}Tc-Kanamycin in Mice (*Mus musculus*)	37-43
Galuh Yuliani, Nur Fitriah Rachmi, Budiman Anwar	Colour Removal of a Model Pulp Mill Effluent using Coagulation and UV- Oxidation	44-48
Yuli Rohyami, Julia Rahayu	Spectrophotometric Determination of Iron(II) and Iron(III) in Well Water	49-55
Irfany A., Permanadewi S., Aladin S., Saprudin D.	Ekstraksi Unsur Tanah Jarang dari *Tailing* Pasir Timah	56-63
Isti Daruwati, Maula Eka Sriyani, Teguh Hafiz Ambar Wibawa, Misyetti	Uncertainty Estimation on Radiochemical Purity Determination of ^{99m}Tc-CTMP Labeled Compound	64-71
Kris Tri Basuki	Effect of Injection Time and Concentration and pH On The Existence of Ozone Bacterium Escherichia Coli Process With Ozonation Disinfection of Drinking Water	72-81
Kris Tri Basuki, M. Santoso, N. Muhayati	Neutron Activation Analysis Application For Determination of Microelements Foodstuffs In Central Java	82-90
Manihar Situmorang and Isnaini Nurwahyuni	Amperometric Biosensor for the Dertemination Cholesterol in Traditional Food Samples	91-99
Muhayatun, Diah Dwiana Lestiani, Syukria Kurniawati, Woro Yatu Niken	Multi Elemental Characterization of Coal by Instrumental Neutron Activation Analysis and X-Ray Fluorescence	100-106
Mulyono Daryoko, Yuli Purwanto	Calculation of Radioactive Waste in the Graphite Thermal Column of the Kartini Reactor, when Carried Out Decommissioning	107-115
Noer Komari, Radna Nurmasari, Ika Noormeidasari	Optimization on Column in Adsorption of Cr (VI) by Eichhornia crassipes Biomass	116-122
Peristiwan Ridha Widhi Astana and Agus Triyono	Clinical Observation of Jamu Formula for Haemmorhoid Treatment	123-128
Poppy Intan Tjahaja, Putu Sukmabuana, Neneng Nur Aisyah	Extraction of ^{134}Cs from Soil Using EDTA and DTPA Chelating Agents: A Soil Column Study	129-137
Qonitah Fardiyah, Akhmad Sabarudin, Mahani Daninda	Fabrication and Characterization Coated Wire Lead (II) Ion Selective Electrode (ISE) Based on Pyrophyllite	138-144
Reni Banowati Istiningrum, Christny Desiree Tiwow, Satya Candra Wibawa Sakti, Nuryono	Synthesis of Quaternary Ammonium Modified Silica Gel from Rice Husk	145-154
Riyanto	Synthesis and electrochemical characterization of Nickel-Cobalt Porous Electrode	155-162
Slamet Sumardi, Fika Rofiek Mufakir, Nurbaiati Marsas	The effect of Sulfuric Acid Concentration and Temperature On leaching Low Grade Manganese Ore in Way Kanan Lampung	163-170
Solihin	Leaching Behaviour of Low Grade Lateritic Ore For Sulawesi	171-176
Sri Adelila Sari, Fajrina Humayra	Qualitative Determination of Formalin in Salted Fish from Traditional Markets, Banda Aceh	177-185
Syukria Kurniawati, Nasjilah Muhayati, Muhayatun Santoso,	Application of NAA for Fe and Zn Determination in Foodstuffs from Several Cities in Central Java	186-193

Diah Dwiana Lestiani, Endah Damastuti		
Umi Laila, Sri Pudjiraharti, Een Sri Endah	The Opportunity of Zeolite, Bleaching Earth, and Granular Activated Carbon as Difructose Anhydride III Decolorization Agent	194-199
Wahyu Perdana Wuryaningsih, Maria Christina Prihatiningsih, Isti Daruwati	Penandaan M41S-NH_2 dengan Radionuklida Teknesium-99m Menggunakan Ko-ligan Pirofosfat dalam Aplikasi Radiosinovektomi	200-208
Zainus Salimin, Pungky Ayu Artiani, and Endang Nuraeni	Utilization of Immobilized Extracellular Polymeric Substance on Epoxy Polymer for Removing of Chromium	209-221
Harry Cahyono, Hanik Humaida, Sri Hartiyatun	Penyelidikan Geokimia Gunung Slamet 2012	222-232
Ratih	Matrix Interferences Study in Solution Containing Arsenic, Cadmium and Lead by ICP-AES	233-238
Gunandjar, Titik Sundari, Yuli Purwanto	The Immobilization of Uranium Radioactive Waste Using Matrix Material of Titanate and Phosphate Supercalcine Synrocs	239-253
Andika Bayu Aji, Suryono, Harry Cahyono, Sri Hartiyatun	Geochemical Investigation of Water and Volcanic Gas at Mount Wilis' Slope	254-262
Yeanchon H. Dulanlebit and M. Bachri Amran	Development of Analysis Method for Iodine Based on Flow Injection Analysis	263-273
Atikah, Rizki Layna R, Rizka Setianing Wardhani	Zeolite Carbon Composite Polyvinyl-Coated Wire Electrode Asiodine Sensor to Detect Iodine Deficiency Disorders	274-280
Julius Pontoh	Brown Sugar Color for the Sugar Quality Assessment	281-288
Retno Ariadi Lusiana, Dwi Siswanta, Mudasir	Study of Urea and Creatinine Transport Through N-Carboxymethyl Chitosan/Poly Vynyl Alcohol (N-CMC/PVA) Blend Membrane	289-297
Widodo B., Ribut L, Kasam, Ike Agustina	Domestic Waste Reduction Strategies for Code River Pollution in Yogyakarta Special Region	298-310
Pravil M. Tambunan, Hamonangan Nainggolan, Jamahir Gultom,	The Study of pH and Minerals Fe, Ca, Mg and Cl Effects on Growth of Koi (*Cyrpinus carpio*) in Aquarium Filled by River Tuntungan Water	311-317
Akbarningrum Fatmawati, Yusnita Liasari, Tjie Kok	Effect of pH and Fermentation Time on the Biohydrogen Production from Sugar Cane Molasse	318-324
Kun Sri Budiasih, Chairil Anwar, Sri Juari Santosa, Hilda Ismail	Molybdenum Complexes with Amino Acids as Antihyperglicemic Agent : Preparation and Spectroscopic Studies*)	325-331
Johnly Alfreds Rorong	Analysis of Ferrous Ion Species in Agriculture Waste as Biosensitizer in Iron Photoreduction Process	332-342
Bakhadir Rismetov, Tribidasari A. Ivandini, Endang Saepudin, Yasuaki Einaga	Development of an Immunochromatographic Strip Test and electrochemical detection of melamine using Platinum deposited Boron-Doped Diamond (BDD) electrode	343-350
Tresye Utari, Yoki Yulizar, Dedy Mahardika	Banana Peel-Nanochitosan Biocomposite for Pb(II) Ions Removal from Industrial Wastewater	351-356
Itmi Hidayat Kurniawan, Sahat Simbolon, Indah Soesanti	Spectral Detection and Measurement System for Emition Spectrograph Analysis with Digital Image Processing	357-368

Proceeding
The 2nd International Conference of the Indonesian Chemical Society 2013
October, 22-23th 2013

Graphene Supported Oxide Systems for Catalytic Oxidation of Organic Compounds in Aqueous Solution for Water Treatment

Shaobin Wang, Stacey Indrawirawan, Yunjin Yao, Hongqi Sun

Department of Chemical Engineering, Curtin University, GPO Box U1987, Perth WA 6845, Australia

Introduction

Organic contaminants in water have been a big group of pollutants which are toxic and persistent. Presently, a great development has been achieved in decomposing these organic pollutants in wastewaters by advanced oxidation processes (AOPs), involving various chemical, photocatalytic, electrocatalytic methods.Among various techniques of catalytic oxidation for water and wastewater treatment, Fenton reaction is one of the cost-effective technologies where hydroxyl radicals (•OH) are usually main highly reactive oxidizing species generated to degrade organic contaminants. Similar to the activity of hydrogen peroxide for the degradation of organic pollutants, alternative oxidants such as peroxymonosulphate (PMS) have been found to be highly effective in chemically mineralizing various organic contaminants.

Graphene, a single layer of carbon atoms tightly packed into a two-dimensional honeycomb sp^2 carbon lattice, possesses a large surface area, open porous structure, flexibility, chemical stability, and very high electrical conductivity, which warrant it as a good candidate for constructing graphene-based composite materials with metal oxides. Here, we present synthesis of metal oxides (Co_3O_4 and $CoFe_2O_4$) and reduced graphene oxide (rGO) via a chemical deposition of Co_3O_4 and $CoFe_2O_4$ NPs onto GO, followed by reduction of GO to graphene in hydrothermal solution.These composites were tested in the catalytic performance in heterogeneous activation of peroxymonosulfate (PMS) for decomposition of phenol.

Experimental

GO was synthesized using the Hummers method through oxidation of graphite powder. In a typical synthesis of the Co_3O_4-rGOand $CoFe_2O_4$–rGO hybrids, firstly, cobalt and iron precursor were dispersed in distilled water, and GO was dispersed in 250 mL water by sonication for 2 h to achieve uniform dispersion of GO. Then, precursor solution was gradually added to the GO solution. Meanwhile, ammonia (28%) or NaOH solution was added to the above solution, which will be used for precipitation and GO reduction. Finally, the mixture was transferred into an autoclave for hydrothermal treatment at 180 ℃ under static condition for 12 h. The solid product was separated by centrifugation, washed thoroughly with water and absolute ethanol to remove any impurities.

The crystallographic structure of the catalysts was investigatedon a Bruker D8-Advance X-ray diffractometer with Cu Kα radiation (λ = 1.5418 Å), with accelerating voltage and current of 40 kV and 40 mA, respectively. FT-IR spectra were recorded on a Perkin-Elmer Spectrum 100 with a resolution of 4 cm^{-1} in transmission mode at room temperature. The morphology of the materials were characterized by FESEM (Zeiss Neon 40EsB FIBSEM) equipped with EDS and TEM (JEOL 2011 TEM). TGA was performed by heating the samples in an air flow at a rate of 100 mL/min using a Perkin-Elmer Diamond TG/DTA thermal analyzer with a heating rate of 10 ℃/min. The surface area, total pore volume, and pore size distribution of all samples were determined by N_2 adsorption at -196 ℃ using Autosorb (Quantachrome Corp.). All samples were degassed at 100 ℃ for 4 h, prior to the adsorption experiments. The Brunauer-Emmett-Teller (BET) surface area and pore volume were obtained by applying the

BET equation and p/p_0=0.95 to the adsorption data, respectively. The pore size distribution was obtained by the Barrett-Joyner-Halenda (BJH) method.

To study the activity of the catalytic oxidation of phenol, batch experiments were carried out in a 150 mL batch reactor. All reactions were initiated without the pH being controlled by mixing appropriate concentrations of phenol, oxone and a catalyst. Fixed amount of oxone was added to a phenol solution and allowed to dissolve before the reaction. Later, catalysts were added to start the reaction. The reaction was carried on for 1 h and stirred at different temperatures (25, 35 and 45 ℃). At predetermined time intervals, 0.5 mL liquid was withdrawn using a syringe filter into a HPLC vial, and 0.5 mL of methanol was added to quench the reaction. The concentrations of phenol were analyzed using a HPLC with a UV detector at the wavelength of 270 nm. The column used was C-18 and the mobile phase was solution of 30% CH_3CN and 70% water.

Results and discussion

The phase structure of as-synthesized samples was firstly determined by XRD. The results indicate that the hybrids consist of disorderedly stacked graphene sheets and well crystallized Co_3O_4 or $CoFe_2O_4$. The average crystallite sizes of Co_3O_4 in Co_3O_4–rGO and $CoFe_2O_4$ NPs in $CoFe_2O_4$–rGO were estimated to be 32.7 and 23.8 nm, respectively, which were consistent with the TEM observations (Fig.1).According to the TGA analysis, mass loss in Co_3O_4–rGO and $CoFe_2O_4$–rGO showed about 58% and 63.6 wt% of metal oxide deposited on the surface of graphene.

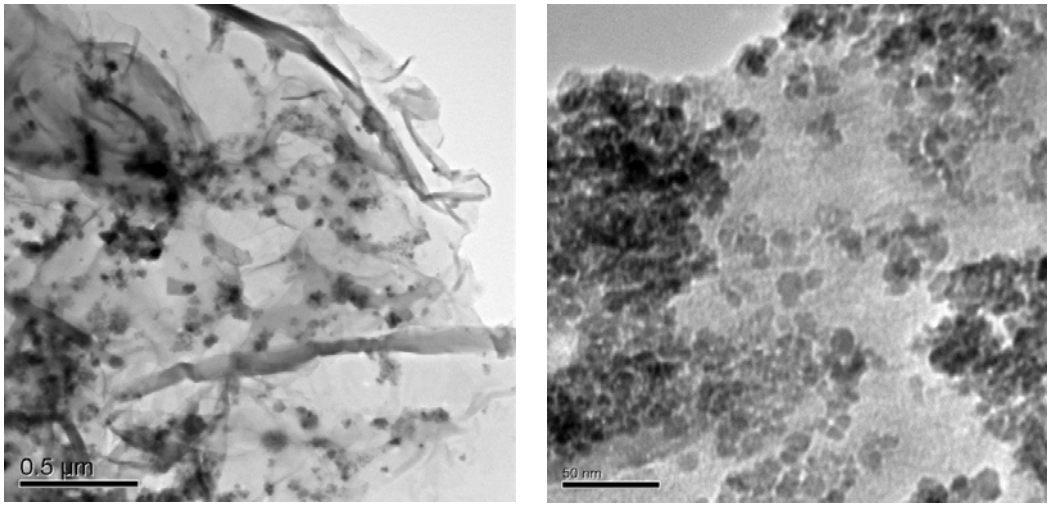

Fig. 1TEM images of Co_3O_4–rGO and $CoFe_2O_4$–rGO.

The catalytic performances of rGO, Co_3O_4,$CoFe_2O_4$, Co_3O_4–rGO and $CoFe_2O_4$–rGO hybrids in the catalytic oxidation of phenol in the presence of PMS are shown in Figure 2. Nearly 23% of phenol (20 mg/L) was removed in 60 min in the presence of rGO, suggesting minor reaction of phenol degradation could occur. For pure Co_3O_4 sample, 100% of phenol was removed in 60 min while for $CoFe_2O_4$ sample, 51% of phenol was removed in 60 min. meanwhile the degradation rate of phenol with $CoFe_2O_4$–rGO and Co_3O_4–rGO hybrids was extremely fast and took around 30 and 20 min, respectively,for complete phenol oxidation under the same conditions.

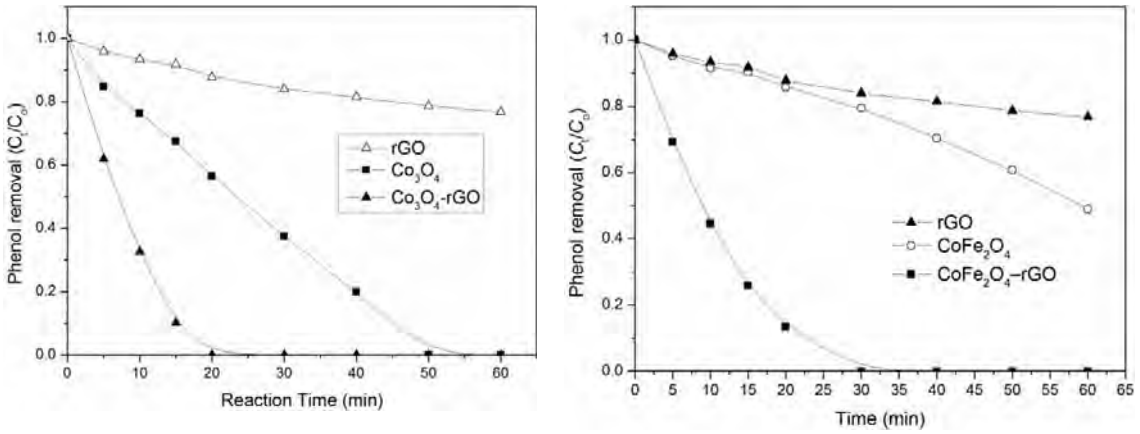

Figure 2. Phenol degradation using different catalysts (Reaction conditions: [Phenol] = 20 mg/L, [PMS] = 0.3 g/150 mL, [Catalyst] = 10 mg/150 mL)

The catalytic performance of Co_3O_4–rGO/PMS and $CoFe_2O_4$–rGO/PMS at different temperatures are shown in Figure 3.As can be seen the rate of disappearance of phenol increased at increasing temperature.It was found that phenol degradation in Co_3O_4–rGO/PMS process is well formulated by the pseudo-zero-order kineticsand that $CoFe_2O_4$–rGO/PMS process is well formulated by the pseudo-first-order kinetics.The activation energy (Ea) values for Co_3O_4–rGO and $CoFe_2O_4$–rGO were obtainedas 26.5 and 15.8 kJ mol^{-1}, respectively.

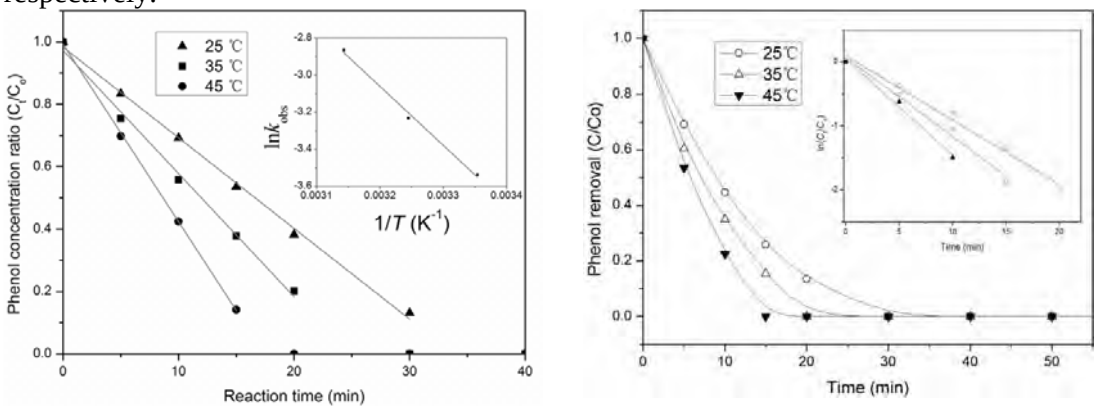

Figure 3. Effect of reaction temperature on phenol degradation using Co_3O_4–rGO/PMS and$CoFe_2O_4$–rGO/PMS.

Acknowledgement
The authors are grateful to the China Scholarship Council and CRC CARE for financial supports.

References

1. Sie King Ling, Shaobin Wang, Yuelian Peng, *J. Hazard. Mat.*, 2010, 178, 385-389.
2. Yunjin Yao,Zeheng Yang, Hongqi Sun, Shaobin Wang, *Ind. Eng. Chem. Res.*, 2012,51, 14958−14965.
3. Yunjin Yao, Zeheng Yang,Dawei Zhang, Wenchao Peng, Hongqi Sun, Shaobin Wang,*Ind. Eng. Chem. Res.*, 2012, 51, 6044-6051.

Proceeding
The 2nd International Conference of the Indonesian Chemical Society 2013
October, 22-23th 2013

Chemistry and biology of brominated compounds from marine algae *Laurencia* spp.

Tatsufumi Okino

Faculty of Environmental Earth Science, Hokkaido University, Sapporo, 060-0810, Japan
(okino@ees.hokudai.ac.jp)

Fouling organisms such as barnacles and mussels cause decrease of fuel efficiency of ships. Antifouling coatings are urgently needed to prevent fouling organisms, to reduce carbon dioxide emissions from ships, and to prevent invasive organisms. Especially international treaty of the International Maritime Organization (IMO) to ban the use and existence of ship's hull of organic tin compounds as antifouling agents went into effect in 2008. A number of antifouling marine natural products have been reported in the past decade. Previously we screened marine invertebrate for antifouling against barnacle larvae. As a result, we found several antifouling compound such as isocyano compounds. For example, 10-isocyano-4-cadinene (**1**) is one of potent compounds, of which total synthesis was completed recently. In addition, 3-isocyanotheonellin (**2**) was explored as a leading compound. Over 90 compounds were synthesized and one of them was selected for the field test. Since the result was promising, we are currently collaborating with a paint company to pursue industrial application. Also their mode of action is being studied.

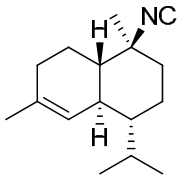

1

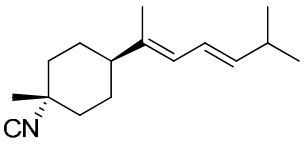

2

Recently we screened marine algae for antifouling activity against barnacle larvae using *Amphibalanus amphitrite*. Especially we focused on red algae *Laurencia* spp., because they have precedent antifouling compounds. For example, elatol is a well-known example, but it was not pursued in industry due to its toxicity. Laurinterol is another example. We found laurinterol acetate (**3**) is more active (EC_{50} = 0.37 g/mL). A triterpenoid, thyrsiferol (**4**) also showed a potent antifouling activity (EC_{50} = 0.11 g/mL).

ISBN: 978-979-96595-4-5

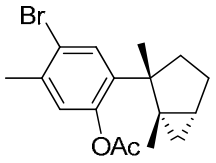

3

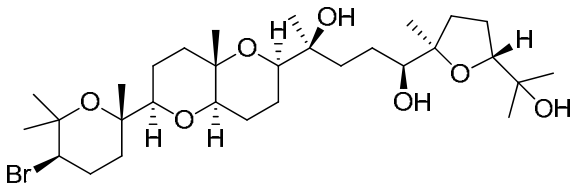

4

A new compound, omaezallene (**5**) showed EC_{50} of 0.22 g/mL and LC_{50} of 3.4 g/mL against barnacle larvae. Determination of planar structure of omaezallene was straight forward by comparing spectroscopic data with literature data of a known bromoallene. Absolute configuration of bromoallene moiety was predicted by Lowe's rule. Lowe's rule is an empirical rule to predict absolute configuration of simple allenes, which was applied for fungal metabolite, diyneallene moiety containing compounds. If the optical rotation is positive, allene is *S*. If negative, allene is *R*.To clarify relative configurations of other parts, omaezallene was derivatized into an acetonide. NOESY experiments of the acetonide indicated relative configurations of other chiral centers except C-9. Total synthesis of proposed structure was achieved by using D-glucose as a starting material. Both epimers at C-9 were synthesized. Comparison of NMR data and optical rotation concluded all absolute configurations of omaezallene. Interestingly epimers of C-9 showed opposite sign of optical rotation. All bromoallenes which were isolated from *Laurencia* so far followed Lowe's rule. 9-*epi*-omaezallene is only exception. In fact, Lowe mentioned that the rule could not be applied if the substituent of bromoallene contained configurational asymmetry.

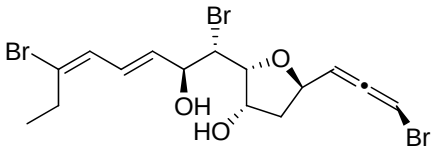

5

The well-known acetogenin, laurencin from *L. nipponica* also showed potent antifouling activity against barnacle larvae (EC_{50} = 0.23 g/mL), but did not show any toxicity even at 100 g/mL. We tested ecotoxicities of laurencin against the copepod *Tigriopus japonicus*, the water flea *Daphnia magna*, the medaka *Oryzias latipes* juveniles and the clown fish *Amphiprion ocellaris* larvae and juveniles. These toxicities of laurencin were 10 – 100 times weaker than those of currently available antifouling agent copper pyrithione.

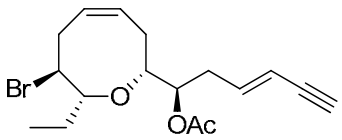

6

Laurencia is one of the richest producers of brominated secondary metabolites. Biosynthesis of brominated compounds such as laurencin, have been studied since late 1990s. Nevertheless, it remains poorly understood. We conducted cDNA cloning and heterologous expression of vanadium dependent bromoperoxidase (VBPO) from *L. nipponica*. Properties of recombinant enzymes were characterized. In addition, bromination activity to a proposed natural precursor of laurencin was observed. The results suggest that VBPOs are pivotal candidates of biosynthetic enzymes that catalyze the bromination of secondary metabolites in*Laurencia* spp.

ISBN: 978-979-96595-4-5

Proceeding
The 2nd International Conference of the Indonesian Chemical Society 2013
October, 22-23th 2013

Chlorophyll and Carotenoid Prospects on Food, Health and Energy

Heriyanto and Leenawaty Limantara*

*Ma Chung Research center for Photosynthetic Pigments
Universitas Ma Chung
Villa Puncak Tidar N-1 Malang, East Java, Indonesia,
*email: leenawaty.limantara@machung.ac.id

Abstract

Indonesia is rich in biodiversity with the abundant natural resources. Most of Indonesia natural resources, i.e. plant, algae, microorganism, have potency as pigment sources. Chlorophyll (Chl) and carotenoid (Crt) are the main pigments in photosynthesis process and have been known to be responsible for health benefits as antioxidant, pro-vitamin A, anti-cancer, anti obesity, etc., and also natural colorants. Basic experiments of Chl and Crt, that is extraction and purification of pigment, content of pigment, composition of pigment, chemical and physical properties of pigment, have been extensively investigated to get fruitful experimental results for the prospect of these pigments. Three prospects of Chl and Crt are pigment on food, health, and energy. The prospect of pigment on food applies Chl and Crt as natural food colorants which have additional health benefits. Pigment on health utilizes Chl and Crt for better health and improved quality of life such as Vitamin A deficiency (VAD), and iron deficiency anemia (IDA). Another subject of this prospect is invention and improvement of stable Chl-based photosensitizer in photodynamic therapy for cancer and tumor. The last prospect of Chl and Crt is for energy. Optimization of design principle of natural systems in light harvesting, energy transfer and energy conversion could be used for the next generation of solar cells.

Keywords: chlorophyll, carotenoid, antioxidant, pro Vitamin A, anti cancer, anti obesity, photosensitizer, solar cell

Introduction

Photosynthesis is a fundamental process for living organisms. Chlorophyll (Chl) and carotenoid (Crt) are photosynthetic pigments which play important roles in this process (Telfer *et. al.*, 2008; Berera *et. al.*, 2009). The former pigment performs a light harvesting (LH) role and serves to funnel absorbed solar radiation to reaction center where photochemical reaction occurs. The latter is also involved in LH and plays photo-protective roles by quenching Chl triplet state and scavenging singlet oxygen. These pigments are naturally found in photosynthetic organisms, for example plant, bacteria, and algae which abundantly occur in Indonesia natural resources. In addition, Crt is present in human and animal as well (Gross, 1991). Britton *et. al.*, (2004) listed more than 700 known naturally occurring Crts that have been isolated from natural resources. The major Crts, that is beta-carotene (β-carotene), fucoxanthin, bixin, crocin, safranal, lycopene,

lutein, zeaxanthin and asthaxanthin, are well known as provitamin A, food colorant, antioxidant, etc.

The functions and abundance of these pigments in nature attract us to perform comprehensive experiments from basic to applied fields. Experiments in the basic level have been conducted to gain fruitful information for the next steps of experiments. Limantara *et. al.*, (1994; 1996) applied a series of isotopes-labelled bacteriochlorophyll (BChl; Chl form in photosynthetic bacteria) to determine the excited states of BChl. The invention of BChl excited states has an important contribution to the usage of BChl and its derivatives as photosensitizers in photodynamic therapy (PDT) for cancer and tumor treatments (Limantara *et. al.,* 2006). Other basic experiments on chemical and physical properties of BChl and its derivatives, such as: photostability (Limantara *et. al.,* 2006; Susanti *et. al.,* 2007; Limantara and Heriyanto, 2010b), aggregation, coordination state, and pH effect (Limantara *et. al.,* 1997; *Koyama et. al.,* 2006; Santosa *et. al.,* 2008; Heriyanto *et. al.,* 2009) were carried out to determine the best photosensitizer.

Material and Method

Photosynthetic organisms, i.e. indigenous plants, macroalgae, microalgae, photosynthetic bacteria, were used as samples for Chl and Crt experiments. The screening of potential Indonesian natural resources as pigment sources was conducted based on the pigment content, tha is relatively Chl content of leaves was determined by portable chlorophyll meter (Rahayu and Limantara, 2005; Heriyanto and Limantara, 2006b) and nitrogen meter (Tantono *et. al.*, 2013), in vitro Chl and Crt contents were determined from crude pigment extracts by spectrophotometry (Madalena *et. al.*, 2007) and high performance liquid chromatography (HPLC) (Limantara and Heriyanto, 2010a) methods; and pigment composition was determined by thin layer chromatography (TLC) (Heriyanto and Limantara, 2006a) and HPLC (Limantara and Heriyanto, 2010). Column chromatography and HPLC were applied for pigment purification (Sukoso *et. al.*, 2010; Pringgenies *et. al.,* 2011) then the purified pigment was identified by UV-Vis spectrophotometer, TLC, HPLC, and nuclear magnetic resonance (Limantara *et. al.,* 1995; Sukoso *et. al.,* 2010). Tests of pigment stabilities against thermal and irradiation treatments (Heriyanto and Limantara, 2010b; Wijaya *et. al.,* 2010; Prihastyanti *et. al.,* 2010) and pH values

effect (Heriyanto *et. al.*, 2004; Kusmita and Limantara, 2009;) were performed for the purified pigment and crude pigment extract.

Biopigment research

Sources of major pigments have been well recognized, that is carrot (contain(s) β-carotene), tomato (lycopene), brown seaweed (fucoxanthin), photosynthetic bacteria (BChl a), leafy vegetable and *Chlorella sp*. (Chl a), saffron '*Crocus sativus*' (crocin and safranal), *Bixa orellana* (Bixin), salmon fish and *Haematococcus pluvalis* (astaxanthin). Rahayu and Limantara (2005) revealed that *katuk* (*Sauropus androgynus*) and *suji* (*Pleomele angustifolia* N.E. Brown) leaves have relatively high Chl content from several green leafy plants. Fucoxanthin is known as the main Crt in brown seaweed and *Padina australis* has the highest fucoxanthin content from 5 species of brown seaweed (Limantara and Heriyanto, 2010). Optimization of fucoxanthin extraction efficiency by several organic solvents in *P. australis* was done by Limantara and Heriyanto (2011a) and methanol was the best solvent for fucoxanthin extraction. Indrawati *et. al.*, (2010b) did a similar experiment for simultaneus BChl and Crts extraction in *Rhodopseudomonas palustris*. Some experiments on pigment composition have been conducted for brown seaweeds (Limantara and Heriyanto, 2010; Indrawati *et. al.*, 2010a), *Kappaphycus alvarezii* (de Fretes *et. al.*, 2011), leafy plant (Christanti *et. al.*, 2011), palm oil (Syahputra *et. al.*, 2008). Chl a is the dominant Chl in brown seaweeds, *K. alvarezii*, leafy plant, while fucoxanthin, zeaxanthin, lutein are their main Crts, respectively. Syahputra *et. al.*, (2008) concluded that β-carotene is the main Crt in palm oil. Lycopene, neurosporene, γ-carotene, β-carotene and phytoene are Crts of *Neurospora Intermedia* which is purified from Indonesian fermented peanut cake (Priatni *et. al.*, 2010).

Chl *a* is unstable pigment towards acid, temperature, and light (Gross, 1991). The addition of other compounds as Chl *a* protector and chemical modifications of Chl *a* could improve its stability. Kartikaningsih *et. al.*, (2010) used fucoxanthin as a photoprotector for Chl *a* against irradiation treatment. Absorption spectra of Chl *a* and fucoxanthin in acetone are shown in Figure 1a. Intensity of Qy band (at 662 nm) of Chl *a* decreased after Chl *a* solution was exposed to the light. Decreasing this intensity of Chl *a* (Figure 1b) was bigger than that of mixture of Chl *a* and fucoxanthin (Figure 1c). This result indicates the photoprotection function

ISBN: 978-979-96595-4-5

of Crt. Photoprotection function of β-carotene and lutein against Chl *a* was investigated by da Costa *et. al.*, (2007). Chemical modifications of Chl *a* at its central metal and peripheral chains to be chlorophylin increased its solubility in aqueous solution and its stability (Sumpana, 2013).

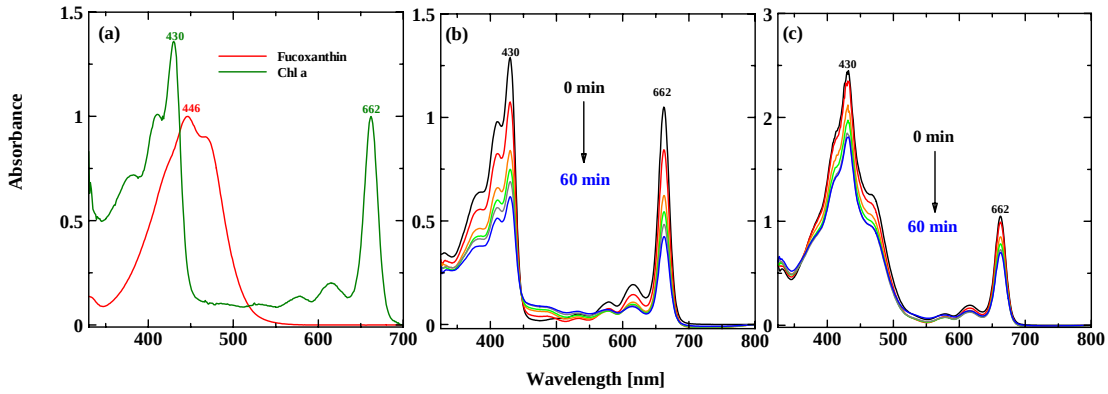

Figure 1. Absorption spectra of fucoxanthin and Chl a in acetone (a), photostability tests of Chl *a* (b), mixture of fucoxanthin and Chl *a* (1:1, mol/mol) (c) during irradiation treatment for 60 minutes.

Application of pigment on food, health and energy

Ingested Chl and Crt are directly obtained from natural food especially vegetables and fruit. In their development, these pigments are applied to food industry as natural food colorants. Chl and Crt have been proven to have health benefits as antioxidant, anti-cancer, anti-inflammation, anti-obesity, pro-vitamin A, and in age-related degenerative diseases. Therefore Chl and Crt are highly potential to be used as healthy food ingredients and functional food. In Indonesian traditional snacks, pigment extracts from *P. angustifolia* and *pandan* (*Pandanus amaryllifolius* Roxb.) leaves are commonly used for natural green colorant. Recently, Arifin (2013) made prototype of natural green food colorant powders and investigated their stabilities and pigment composition. The addition of *Chlorella pyrenoidosa* and *Monascus purpureus*, which is rich in pigments, into the tea as functional drink increased the antioxidant activity and acceptability by the panellist (Megawati *et. al.*, 2013). In addition, the occurrence of red colour in red palm oil, coming from Crts, is becoming the healthful choice for oil cooking.

Indonesia has been known as the world's largest exporter of crude palm oil (CPO) and also one of the most important exporters of seaweeds and some of decapods crustaceans. However, these natural resources have not been maximally exploited as the source of β-carotene,

astaxanthin, fucoxanthin, Chl, etc., which are important for maintaining healthcare. Astaxanthin is a potential antioxidant, because of this Crt has the strongest antioxidant activity compared to other natural antioxidants, such as: vitamin E and β-carotene (Shimidzu *et. al.*, 1996 ; Bagchi, 2001). Therefore, astaxanthin is used as cosmetic ingredient due to its antioxidant and photo-protector functions (Andyka *et. al.*, 2013). Herbal medicine containing *P. australis* and *Sprirulina platensis*, which contain fucoxanthin, lutein, Chl *a* and Chl *b* as dominant pigments, showed anti-atherosclerotic (Indrawati *et. al.*, 2013). The potency and efficacy of astaxanthin as anti-cholesterol was reviewed by Wijaya *et. al.*, (2013). PDT is photo-chemotherapy combining the use of light, oxygen and photosensitizer. Recently, there are a number of efforts to invent and develop the stable Chl-based photosensitizer in PDT for cancer and tumors. Zn-pheophorbide *a* is a very promising low-cost, synthetically easily accessible, second generation photosensitizer against human cancer (Jakubowska *et. al.*, 2013).

There are increasing numbers of pigment application to energy utilization especially solar cells. Dye-sensitized solar cell (DSSC) is one technology of solar cells which mimics a basic principle of photosynthesis (Heriyanto and Limantara, 2010a). Synthetic dyes, i.e. ruthenium complexes, are commonly applied to this solar cell as sensitizers for gathering solar energy with the conversion efficiency of sunlight to electric power up to 11% (Gratzel, 2004). Besides the usage of synthetic dyes, photosynthetic pigments, that is Chl and its derivatives (Tributsch and Calvin, 1971; Wang *et. al.*, 2010), Crts (Wang *et. al.*, 2005; Yamazaki *et. al.*, 2007), have been used as sensitizers with a low cost, although their values of the conversion efficiency are lower than the use of synthetic dyes. Currently, bio-hybrid solar cells, a novel photo-nano-device, have been constructed from LH complexes of photosynthetic bacteria on metal surface. Plasmon excitation in metallic nanoparticles provide an excellent way to control the optical properties of matter and enhance the productive photochemistry of the LH complexes (Bujak *et. al.*, 2011 and 2012). Fiedor *et. al.*, (2004) and Akahane *et. al.*,. (2004) modified native LH complexes by reconstitution approach to enhance the efficiency of singlet energy transfer from Crt to BChl.

Acknowledgement

The financial support from the Directorate of Higher Education, Ministry of Education and Culture (National strategic grant number 182/SP2H/PL/Dit.Litabmas/V/2013) and Ministry of Research and Technology (Sinas grant number 187/M/Kp/XI/2012) are greatly appreciated.

References

Akahane, J., Rondonuwu, F.S., Fiedor, L., Watanabe, Y., and Koyama, Y. (2004). Dependence of singlet-energy transfer on the conjugation length of carotenoids reconstituted into the LH1 complex from *Rhodospirillum rubrum* G9. Chem. Phys. Lett., 393: 184-191.

Andyka, M.I.R., Brotosudarmo, T.H.P. and Limantara, L. (2013). Utilization of Aloe vera gel and astaxanthin as active ingredients in cosmetics. Proceedings of 2nd Natural Pigments Conference for South-East Asia (NP-SEA), Malang, July 12-13, 2013.

Arifin, V. (2013). Studi komposisi dan stabilitas pigmen pada prototype serbuk pewarna makanan hijau alami daun pandan wangi (*Pandanus amaryllifolius* Roxb.) dan suji (*Pleomele angustifolia* N.E. Brown). Skripsi Teknik Industri, Universitas Ma Chung, Malang.

Bagchi, D. (2001). "Oxygen Free Radical Scavenging Abilities of Vitamins C, E, B-Carotene, Pycnogenol, Grape Seed Proanthocyanidin Extract, Astaxanthin and BioAstin in Vitro." On file at Cyanotech Corporation.

Berera, R., van Grondelle, R., Kennis, J.T.M. (2009). Ultrafast transient absoption spectroscopy: principles and application to photosynthetic systems. Photosynth. Res., 101: 105-118.

Britton, G., Liaaen-Jensen, S., and Pfander, H. (2004). Carotenoids: Handbook. Birkhauser, Boston.

Bujak, L., Czechowski, N., Piatkowski, D., Litvin, R., Mackowski, S., Brotosudarmo, T.H.P., Cogdell, R.J., Pichler, S. and Heiss, W. (2011). Fluorescence enhancement of light-harvesting complex 2 from purple bacteria coupled to spherical gold nanoparticle. Appl. Phys. Lett., 99: 173701.

Bujak, L., Brotosudarmo, T.H.P., Czeckowski, N., Olejnik, M., Ciszak, K., Litvin, R., Cogdell, R.J., Heiss, W. and Mackowski, S. (2012). Spektral Dependence of Fluorescence Enhancement in LH2-Au Nanoparticle Hybrid Nanostructures. Acta Physica Polonica A, 122: 252-254.

Christanti, M., Fidelia, A., Heriyanto, Brotosudarmo, T.H.P., and Limantara, L. (2011). Fence Plants – A Study of Photosynthetic Pigments Compositions and Their Crude Extract Photostability. Proceeding of International Conference on Natural Sciences, ISBN 978-3-8440-1403-7. Malang, July 9-11.

da Costa, J.F., Karwur, F.F. dan Limantara, L. (2007). Fotoproteksi beta Karoten dan Lutein terhadap Klorofil a dalam Aseton. Proceeding of National Conference on Back to Nature with Natural Pigment. ISSN: 979-978-89-2. Salatiga, 24 Agustus.

de Fretes, H., Susanto, A.B., Limantara, L., Prasetyo, B., Heriyanto and Brotosudarmo, T.H.P. (2011). Pigment Composition, Photostability and Thermostability Studies of Crude Pigment Extracts from Red, Brown, and Green Varieties of Red Algae *Kappaphycus alvarezii (Doty) Doty*. Proceeding of International Conference on Natural Sciences, ISBN 978-3-8440-1403-7. Malang, July 9-11.

Fiedor, L., Akahane, J., and Koyama, Y. (2004). Carotenoid-induced cooperative formation of bacterial photosynthetic LH1 complex. Biochemistry, 43: 16487-16496.

Gratzel, M. (2004). Conversion of sunlight to electric powder by nano crystalline dye-sensitized solar cells. Journal of Photochemistry and Photobiology A: Chemistry, l64: 314.

Gross, J., 1991. Pigment in Vegetables: Chlorophylls and Carotenoids. New York: Van Nostrand Reinhold.

Heriyanto, Hartini, S. and Limantara, L. (2004). The Content of Chlorophylls, Pheophytins and Pheophorbides in Leaf Mustard (*Brassica juncea* (l.) czern. & coss.) during Processing and Pickled Storage. Proceedings of National Conference on Research, Education and Application of Science, Universitas Negeri Yogyakarta. ISSN: 979-96880-4-3.Yogyakarta, 2 Agustus.

Heriyanto and Limantara, L. (2006a). Komposisi dan Kandungan Pigmen Utama Tumbuhan Taliputri *Cuscuta australis* R.Br. dan *Cassytha filiformis* L. Makara Seri Sains, 10: 69-75.

Heriyanto dan Limantara, L. (2006b). Studi Lapangan Kandungan Klorofil *In Vivo* Daun Cincau Hitam, Cincau Perdu, Cincau Hijau and Cincau Minyak, Journal Natur Indonesia, 9: 41-47.

Heriyanto, Trihandaru, S. dan Limantara, L. (2009). Keadaan Koordinasi dan Proses Agregasi Bakterioklorofil *a* and Turunannya: Studi pada Pelarut Aseton-Air and Metanol-Air, Indo. J. Chem. 9: 113-122.

Heriyanto dan Limantara, L. (2010a). Dye-sensitized solar cell: Teknologi pembentuk sumber energi listrik alternatif. Proceeding of National conference on Technopreneur Day, "Save our earth with green technology". Universitas Ma Chung, Malang, 15 Mei.

Heriyanto and Limantara, L. (2010b). Photo-Stability And Thermo-Stability Studies Of Fucoxanthin Isomerization. Proceedings of Natural Pigments Conference For South-East Asia. ISBN: 978-602-97123-0-8. Malang, 20-21 Maret.

Indrawati, R., Heriyanto, Limantara, L., and Susanto, A.B. (2010a). Study of Pigments Distribution in the Stem, Leaf and Vesicle of *Sargassum filipendula*, *Sargassum polycystum* and *Sargassum sp*. from Madura Waters using High Performance Liquid Chromatography. Proceedings of Natural Pigments Conference For South-East Asia, ISBN: 978-602-97123-0-8. Malang, March 20th-21st.

Indrawati, R., Wijaya, W., Prihastyanti, M. N. U., Heriyanto, Prasetyo, B., and Limantara, L. (2010b). Efisiensi Ekstraksi Bakterioklorofil dan Karotenoid dari *Rhodopseudomonas* palustris dengan berbagai rasio pelarut Aseton dan Metanol. Prosiding Seminar Nasional Sains dan Pendidikan Sains V. ISSN: 2087-0922. Salatiga, 10 Juni.

Indrawati, R., Wijaya, D.E., Indriatmoko, Sulistiawati, E., Suparto, I.H., and Limantara, L. (2013). Hypocholesterolemic effect and pigments composition of herbal medicine containing higher and lower plants. (in Press).

Jakubowska, M., Szczygiel, M., Michalczyk-Wetula, D., Susz, A., Stochel, G., Elias, M., Fiedor, L., and Urbanska, K. (2013). Zinc-pheophorbide a-highly efficient low-cost photosensitizer against human adenocarcinoma in cellular and animal models. Photodiagnosis and Photodynamic Therapy. 10: 266-277.

Kartikaningsih, H., Zaelaniea, K., Puspitasari, F.R., Heriyanto and Limantara, L. (2010). Photo-Stability of Fucoxanthin, Chlorophyll a, Fucoxanthin-Chlorophyl a Mixtures and Crude Pigment Extracts from Brown Algae: Acetone-Water Solvents Study. Proceedings of Natural Pigments Conference For South-East Asia. ISBN: 978-602-97123-0-8. Malang, March 20th-21st.

Koyama, Y., Kakitani, Y., Limantara, L., and Fujii, R. (2006). Effects of Axial Coordination, Electronic Excitation and Oxidation on Bond Orders in the Bacteriochlorin Macrocycle, and Generation of Radical Cation on Photo-Excitation of in vitro and in vivo

Bacteriochlorophyll aAggregates: Resonance Raman Studies. In Advances in Photosynthesis and Respiration. Chlorophylls and Bacteriochlorophylls: Biochemistry, Biophysics, Functions and Applications (Eds: Grimm, B., Porra, R.J., Rüdiger, W., and Scheer, H.). Springer, The Netherlands.

Kusmita, L. dan Limantara, L. (2009). Pengaruh Asam Kuat dan Asam Lemah terhadap Agregasi dan Feofitinasi Klorofil a dan b. Indo. J. Chem. 9: 70-76.

Limantara, L, Koyama, Y., Katheder, I. and Scheer, H. 1994. Transient Raman spectroscopy of ^{15}N-substituted bacteriochlorophyll *a*.an empirical assignment of T_1 Raman lines. Chem. Phys. Lett., 227: 617-622.

Limantara, L., Kurimoto, Y., Furukawa, K., Shimamura, T., Utsumi, H., Katheder, I., Scheer, H. and Koyama, Y. (1995). The Environment of the Four Nitrogen Atoms of Bacteriochlorophyll a in Solutions as Revealed by ^{15}N-NMR Spectroscopy. Proceedings of the Annual Meeting of Japanese Society of Plant Physiologists. In Plant and Cells Physiol. Vol. 36 (Supplement). Shimane University, 29 March.

Limantara, L., Katheder, I., Scheer, H., Schafer, W. and Koyama, Y. 1996. The T_1 and S_1 Raman spectra of ^{15}N and ^{2}H-enriched bacteriochlorophyll *a* : Changes in bond order upon triplet and singlet excitation. Chem Phys. Lett., 262: 656-662.

Limantara, L., Sakamoto, S., Koyama, Y., and Nagae, H. (1997). Effects of Nonpolar and Polar Solvents on the Q_x and Q_Y Energies of Bacteriochlorophyll a and Bacteriopheophytin a. Photochem. Photobiol., 65: 330-337.

Limantara, L., Koehler, P., Wilhelm, B., Porra, R.J., and Scheer, H. (2006). Photochem Photobiol., 82: 774-780.

Limantara, L., dan Heriyanto. (2010). Komposisi Pigmen dan Kandungan Fukosantin Rumput Laut Cokelat dari Perairan Madura dengan Kromatografi Cair Kinerja Tinggi. Indonesian Journal of Marine Sciences. 15: 23-32.

Limantara, L., dan Heriyanto. (2011a). Optimasi Proses Ekstraksi Fukosantin dari Rumput Laut Cokelat, *Padina australis* Hauck, dengan Pelarut Organik Polar, Indonesian Journal of Marine Sciences.16: 86-94.

Limantara, L., dan Heriyanto. (2011b). Photostability of Bacteriochlorophyll a and Its Derivatives as Potential Sensitizers for Photodynamic Cancer Therapy: The Study on Acetone-Water and Methanol-Water Solvents. Indonesian Journal of Chemistry. 11: 154-162.

Madalena, Heriyanto, Hastuti, S.P. dan Limantara, L. (2007). Pengaruh Lama Pemanasan Terhadap Kandungan Pigmen Serta Vitamin A Daun Singkong (*Manihot esculenta* Crantz) and Daun Singkong Karet (*Manihot glaziovii* Muell. Arg), Indo. J. Chem. 7: 105-110.

Megawati, Brotosudarmo, T.H.P. and Limantara, L. (2013) Analytical assays on product quality, organoleptic and antioxidant activity of functional drinks. Proceedings of 2nd Natural Pigments Conference for South-East Asia (NP-SEA), Malang, July 12-13, 2013.

Priatni, S., Limantara, L., Heriyanto, Singgih, M., and Gusdinar, T. (2010). Identification of Carotenoids in *Neurospora Intermedia* N-1 Isolated from Indonesian Fermented Peanut Cake (Oncom Merah). Proceedings of Natural Pigments Conference For South-East Asia. ISBN: 978-602-97123-8. Malang, March 20th-21st.

Prihastyanti, M., Heriyanto, Trihandaru, S., and Limantara, L. (2010). Photostability Of Crude Pigment Extract From Three Species Of Brown Seaweed Based On Spectrum Pattern And Identifying The Degradation Product Based On HPLC Chromatogram. Proceedings of

Natural Pigments Conference For South-East Asia. ISBN: 978-602-97123-0-8. March 20th-21st, Malang.

Pringgenies, D., Ridlo, A., Indriatmoko, Heriyanto and Limantara, L. (2011). Production of Phenazine Pigments From Marine Symbiotic Bacteria in *Gastropod Cerithidea* sp. with Different Growth Media. Proceedings of The International Conference On Natural Sciences(ICONS). ISBN 978-3-8440-1403-7. Malang, July 9-11.

Rahayu, P. and Limantara, L. (2005). Field Evaluation of In Vivo Chlorophyll Content from Several Green Leafy Plants in Around of Salatiga. Proceedings of National Conference on The Scientific Meeting, FMIPA UI, Jakarta. November 25-26.

Santosa, V., Prasetyo, B., and Limantara, L. (2008). The Effect of Aggregation, Acidification and Incubation of The Spectral Pattern of Pd-Bacteriopheophorbide (Tookad). Eksplanasi, 3: 61-70.

Shimidzu, N., Goto, M., and Miki, W. (1996) Carotenoids as singlet oxygen quenchers in marine organisms. Fisheries science. 62: 134-137.

Sukoso, Kartini Zaelanie, Dadang A. Setiyawan, Heriyanto and Leenawaty Limantara. (2010). Antioxidant Activity Study of Fucoxanthin and Crude Pigment Extracts from Three Species of Brown Algae (*Sargassum duplicatum*, *Sargassum filipendula*, and *Sargassum polycystum*). Proceedings of Natural Pigments Conference For South-East Asia. ISBN: 978-602-97123-0-8. Malang, March 20th-21st.

Sumpana, A.F. (2013) Stabilitas bahan baku dan prototype masker wajah dengan perpaduan *Chlorella pyrenoidosa*-klorofilin dan *Spirulina platensis*-klorofilin. Skripsi Teknik Industri, Universitas Ma Chung, Malang.

Susanti, N. I., Trihandaru, S. dan Limantara, L. (2007). Fotostabilitas Bakterioklorofil a dan Bakteriofeofitin a dalam Pelarut Aseton-Air: Potensi terhadap Terapi Fotodinamika Kanker. Proceedings of National Conference on Back to Nature with Natural Pigment. Magister of Biology, Satya Wacana Christian University. ISSN: 979-978-89-2. Salatiga 24 Agustus.

Syahputra, M.R., Karwur, F.F., and Limantara, L. (2008) Analisis Komposisi dan Kandungan Karotenoid Total dan Vitamin A Fraksi Cair dan Padat Minyak Sawit Kasar (CPO) menggunakan KCKT Detector PDA. Jurnal Natur Indonesia, 10: 89-97

Tantono, C., Adhiwibawa, M.A.S., Prilianti, K.R., Prihastyanti, M.N.U., Limantara, L., and Brotosudarmo, T.H.P. (2013) Mata Daun: a mobile application for measuring chlorophylls and nitrogen content of soybean leaf. Proceedings of 2nd Natural Pigments Conference for South-East Asia (NP-SEA), Malang, July 12-13, 2013.

Telfer, A., Pascal, A., and Gall, A. (2008) *Carotenoids in Photosynthesis. In Carotenoids Volume a: Natural Functions* (eds. Britton, G., Liaaen-Jensen, S., Pfander, H.). Birkhauser Verlag Basel, p. 265-308.

Tributsch, H., and Calvin, M. (1971) Electrochemistry of excited molecules: photo-electrochemical reactions of chlorophylls. Photochem. Photobiol., 14: 95-112.

Wang, X.-F., Xiang, J., Wang, P., Koyama, Y., Yanagida, S., Wada, Y., Hiamada, K., Siasaki, S.-I., and Tamiaki, H. (2005). Dye-sensitized solar cells using a chlorophyll a derivative as the sensitizer and carotenoids having different conjugation lengths as redox spacers. Chemical Physics Letters, 408: 409-414.

Wang, X.-F., Koyama, Y., Kitao, O., Wada,Y., Sasaki, S.-I., Tamiaki, H. and Zhou, H. (2010) Significant enhancement in the power-conversion efficiency of chlorophyll co-sensitized solar cells by mimicking the principles of natural Photosynthetic light-harvesting complexes. Biosens. Bioelectron., 25: 191l-1916.

Wijaya, D.E., Delfiana, Y., and Limantara, L. (2013) The potency and efficacy of astaxanthin pigment as a raw material of canti-cholesterol traditional medicine. Proceedings of 2nd Natural Pigments Conference for South-East Asia (NP-SEA), Malang, July 12-13.

Wijaya, W., Heriyanto, Prihastyanti, M. N. U., Indrawati, R., Prasetyo, B., and Limantara, L. (2010): Termostabilias Bakterioklorofil a pada Ekstrak Pigmen Kasar *Rhodopseudomonas palustris*. Prosiding Seminar Nasional Sains dan Pendidikan Sains V. ISSN: 2087-0922. Salatiga, 10 Juni.

Yamazaki, E., Murayama, M., Nishikawa, N., Hashimoto, N., Shoyama, M. and Kurita, O. (2007). Utilization of natural carotenoids as photosensitizers for dye-sensitized solar cells. Solar Energy, 81: 512-516.

Proceeding
The 2nd International Conference of the Indonesian Chemical Society 2013
October, 22-23th 2013

Nanoscale Pore Space Science for Sustainable Chemistry

Katsumi Kaneko

Research Center for Exotic Nanocarbons, Nagano, 380-8553, Japan
kkaneko@shinshu-u.ac.jp

Abstract

The unique nanoscale pore structures of nanocarbon and high surface area carbon, which induce highly dense adsorbed state, are shown. The superhigh pressure-compression effect and stabilization effect of unstable phase of nanoscale pore spaces are given using the examples of 1D atomically 1D metallic sulfur chain crystals, KI nanocrystals and CH_4, respectively. The quantum fluctuation of light molecules such as H_2 and CH_4 should not be neglected in the nanoscale spaces; the quantum fluctuation induces an evident quantum molecular sieving effect on adsorption in nanoscale pores for their isotopes. The intensive confinement of ions in the nanoscale pore spaces gives rise to a partial desolvation and highly packed structure. These results can contribute to sustainable chemistry.

Keywords: nanoscale pore, metal sulfur, single wall carbon, interfacial solid, desolvation, adsorption, nanoconfinement.

All component carbon atoms of graphene, single wall carbon nanotube (SWCNT), single wall carbon nanohorn(SWCNH), and double wall carbon nanotube (DWCNT) are exposed to the interfaces. Figure 1 shows monolayers on the external and internal wall surfaces of SWCNT; all component carbon atoms can interact with molecules on the external and internal sides. Therefore, these systems are not ordinary solids, but interfacial solids. These carbons can easily vary the local structure depending on the stimuli through the morphological defects.[1)] Activated carbon fiber (ACF) or carbide-derived carbon (CDC) can be also regarded as the interfacial solid, because their surface area is close to that of graphene. These materials have an intensive potential for contribution to interfacial science. At the same time, these carbons except for graphene have nanoscale pores which have the deep interaction potential well for molecules, giving rise to a highly dense adsorbed state in the pore spaces and unique functions due to molecule-molecule and molecule-pore wall collective interactions.

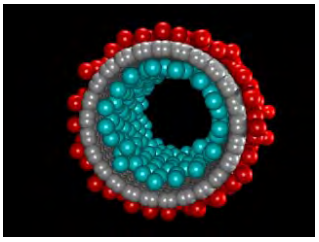

Figure 1. Monolayers on the external and internal tube wall surfaces having opposite sign of nanoscale curvature in SWCNT.

Recently we have obtained clear evidence that confinement of KI nanocrystals below 0.1 MPa induces the solid phase transition into high pressure phase, which occurs above 1.9 GPa for the bulk KI crystals; this remarkable effect is named super high pressure effect.[2)] Thus, phase transition can be influenced remarkably by the nanoconfiment of substances. We measured the rotational-vibration spectra of methane in single walled nanoscale pores near the boiling temperature (111.5 K). The rotational structure almost disappears around 111 K, although the vibration spectrum of methane in the bulk phase has a clear rotational structure. The rotational structure can be observed at 140 K, showing the elevation of boiling temperature of methane adsorbed in the nanoscale tube spaces by 30 K[3)]. Very recently, we obtained intensive evidence on the in-pore superhigh pressure effect of the tubular carbon

spaces. It is well-known that solid sulfur consists of 8-member rings, being insulator. We introduce sulfur vapor below 0.1 MPa in the tubular spaces of SWCNT and DWCNT. High resolution transmission electron microscopic (HR-TEM) observation elucidated the presence of a complete one-dimensional sulfur chain in the tubular space. Figure 2 shows the HR-TEM images of the 1D sulfur chain in the tube spaces of DWCNT whose internal tube diameters are 0.68 and 0.60 nm. The zigzag sulfur chain and complete linear chain are observed in the internal tubes of 0.68 nm and 0.60 nm, respectively. Surprisingly we observed clear X-ray diffraction peaks corresponding to the 1D chain structures of sulfur. [4] This facts indicate that the in-pore superhigh pressure corresponds to 90 GPa at least. In case of Se, a unique helix structure is formed.[5]

The quantum molecular sieving effect is a representative function of the nanoscale pore spaces. The quantum fluctuation difference between light molecules such as H_2 and D_2 is only 0.03 nm at 77 K, leading to an explicit adsorption difference of more than 5 % for H_2 and D_2.[6] The clear adsorption difference of 2 % even between CD_4 and CH_4 was evidenced in the higher fractional filling for 0.7 nm slit-pores. $^{13}CH_4$ and $^{12}CH_4$ can be efficiently separable using the nanoscale pores of SWCNH at 112 K with the quantum molecular sieving.[7] The EXAFS study of Rb^+ ions in the slit pores of ACF indicated partial dehydration.[8] Also organic ion "solution" confined in the slit pores of ACF and CDC was studied with synchrotron X-ray diffraction analysis, providing a highly oriented molecular packing structure.[9]

These carbon nanotube spaces can be electronically modified with the aid of charge-transfer interaction using adsorption of aromatic hydrocarbon molecules. The charge transfer interaction can donate charges to the nanotube walls, changing molecular adsorptivity and dispersion stability in water. Then, these electronically modified SWCNT and/or DWCNT should induce new functions for atoms, ions, and molecules.[10,11]

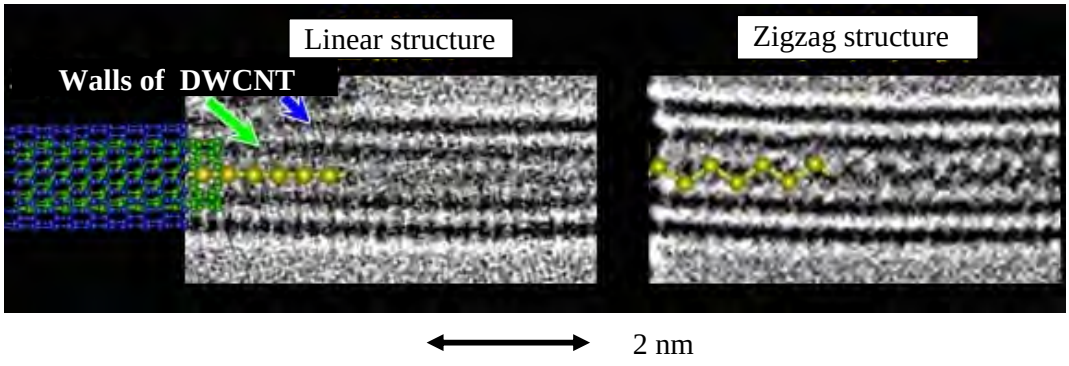

Figure 2. High resolution transmission electron microscopic images of atomically 1-dimensinal metallic sulfur chain crystals in double wall carbon nanotube.

Acknowledgements

K.K. was supported by Exotic Nanocarbons, Japan Regional Innovation Strategy Program by the Excellent, JST. This work was supported by the Grant-in-Aid for Scientific Research (A) (No. 24241038) by JSPS.

References

1) T. Fujimori, K. Urita, D. Tomanek, T. Ohba, I. Moriguchi, M. Endo, K. Kaneko, *J. Chem. Phys.* **136** (2012) 064505-1.
2) K. Urita, Y. Shiga, T. Fujimori, Y. Hattori, H, Kanoh, T. Ohba, H. Tanaka, M. Yudasaka, S. Iijima, I, Moriguchi, F. Okino, M. Endo, K. Kaneko, *J. Amer. Chem. Soc*. **133**(2011) 10344.
3) S. Hashimoto, T. Fujimori, H. Tanaka, K. Urita, T. Ohba, H. Kanoh, T. Itoh, M. Asai, H. Sakamoto, S. Niimura, M. Endo, F. Rodoriguez-Reinoso, K. Kaneko, *J. Amer. Chem. Soc*. **133** (2011) 2022.
4) T. Fujimori, A. Morelos-Gómez, Z. Zhu, H. Muramatsu, R. Futamura, K. Urita, M. Terrones, T. Hayashi, M. Endo, S. Y. Hong, Y. C. Choi, D. Tománek , K. Kaneko,' *Nature Comm*. **4** (2013) 2162.
5) T. Fujimori, R. B. Santos, T. Hayashi, M. Endo, K. Kaneko, D. Tománek, ACS Nano, **7** (2013) 5607.
6) H. Tanaka, D. Noguchi, A. Yuzawa, T. Kodaira, K. Kaneko, *J. Low Temp. Phys*. **157** (2009)352. D.Noguchi, H. Tanaka, T.Fujimori, T. Kagita, Y. Hattori, H. Honda, K. Urita, S. Utsumi, Z.-M. Wang, T. Ohba, H**.** Kanoh, K. Hata, K. Kaneko, *J.Phys.:Condens.Matter*. **22** (2010) 334207.
7) T. Fujimori, D. Minami,T. Tamura, S. Niimura,T. Ohba, T. Itoh, H. Kanoh, K. Kaneko, in preparation.
8) T. Ohkubo, T. Konishi, Y. Hattori, H. Kanoh, T. Fujikawa, K. Kaneko, *J. Am. Chem. Soc.* **124** (2002) 11860
9) A. Tanaka, T. Iiyama, T. Ohba, S. Ozeki, K. Urita, T. Fujimori, H. Kanoh, K. Kaneko, *J. Amer. Chem. Soc.* **132** (2010) 2112. M. Fukano, T. Fujimori, J. Ségalini, E. Iwama, P.-L. Taberna, T. Iiyama, T. Ohba, H. Kanoh, Y. Gogotsi, P. Simon, K. Kaneko , *J. Phys. Chem. C*, ***117*** (2013)5752.
10) F. Khoerunnisa, T. Fujimori, T. Itoh, K. Urita, T. Hayashi, H. Kanoh, T. Ohba, S. Y. Hong, Y. C. Choi, S. J. Santosa, M. Endo, K. Kaneko, dx.doi.org/10.1021/jp303630m | *J. Phys. Chem. C* **116(**2012)11216.
11) F. Khoerunnisa, D. Minami, T. Fujimori, S.Y. Hong, Y.C. Choi, H. Sakamoto, M. Endo, K. Kaneko, *Adsorption*, in press.

Proceeding
The 2nd International Conference of the Indonesian Chemical Society 2013
October, 22-23th 2013

Al_{13} Intercalated and Pillared Montmorillontes from Unusual Antiperspirant Aqueous Solutions: Precursors for Porous Clay Heterostructures and Heptane Hydro-Isomerization Catalytic Activities

Fethi Kooli

Taibah University, Department of Chemistry, POBOX 30002,
Al-Madinah Al-Munawwarah, Saudi Arabia.
E-mail: fkooli@taibahu.edu.sa

We propose to use antiperspirant solution as pillaring agent, containing ACH and other organic modifiers. Montmorillonite clay (Mt) was directly added to an aqueous solution of the antiperspirant dissolved in a certain volume of water at 80 ^{o}C, and at different Al/clay ratios (in weight, R), resulting to Al intercalated Mt precursors (Al-MtR). The amount of Al species incorporated in Al-MtR precursors, depended on the R values, it varied between 8.70 to 19.75 % with a maximum at R value of 12. The pure pillared clays were obtained after calcinations at 500 ^{o}C for R values above 4. For further studies we have selected R value of 6 (Al-Mt6sample).

The thermal stability of Al-Mt6 precursor depended on calcination temperatures. The PXRD patterns indicated that the layered structure was stable up to 800 ^{o}C with a decrease of the 001 intensity's reflection and shrinkage of the basal spacing from 1.94 to 1.72 nm. A complete collapse of the layered structure was achieved at 900 ^{o}C., with an amorphous phase being formed (Figure 1).

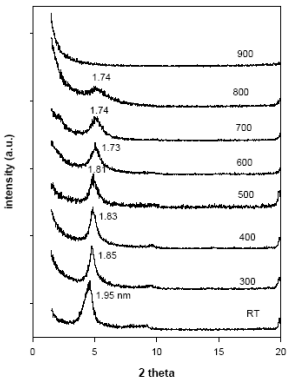

Figure 1. PXRD patterns of Al-Mt6 precursor calcined at different temperatures

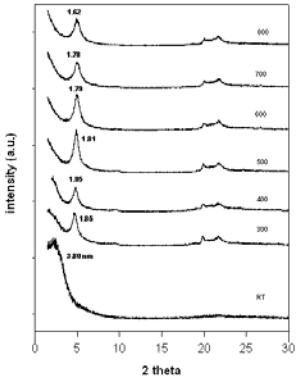

Figure 2. PXRD patterns of PAl-MtCH prepared from Al-Mt6 precursor calcined at different temperatures

^{27}Al-NMR spectral analysis confirmed the presence of Al species in Al-Mt6, with an additional band between 60 and 70 ppm, mostly assigned to the tetrahedral Al from the pillaring species. The position of the Al octahedral peak at 3 ppm shifted to 2.3 ppm. The calcination at 500 ^{o}C resulted to the increase of the tetrahedral peak intensity, with a shift of the octahedral peak at 1.4

ppm, due to the reaction of aluminum species with the Mt sheets. This conclusion was proved by the reaction of the pillared clays with docylamine (C10 amine) solution. After reaction, no expansion of the interlayer spacing was achieved, and it remained constant close to 1.76 nm. Meanwhile, further expansion of the basal spacing was achieved from 1.90 nm to 3.58 nm when the Al-Mt6precursor (no calcined) reacted with C10 amine, and indicated that the intercalated Al species in Mt-Al-6 precursor were easily exchanged with C10 amine molecules.

This finding opened new horizons and the preparation of porous clay heterostructures (PCH) materials was investigated. This method allowed us to minimize the consume of surfactants, by using one directing template (dodecylamine, C12 amine), in order to reduce the organic chemical waste, and to introduce the aluminium species in the mesostructured silica, instead of post grafting in one step reaction, during the preparation of PCH materials.

The synthesis of the PCH samples was achieved by mixing Al-Mt6 precursor or its pillared derivatives with dodecylamine, (C_{12} amine) and TEOS at molar ratios of clay/$C_{12}H_{25}NH_2$/TEOS about 1/20/150. The mixture was stirred for 4 h at room temperature. The organic molecules were removed by calcinations at 550 ^oC in air. The sample is identified as PAl-MtCH. When pillared clays were used, the calcination temperature was added in the sample identification as P-Al-MtXCH,

Figure 2 presents the PXRD of the calcined PCHs, the interlayer spacing of Al-Mt6 increased dramatically from 2.00 nm to 3.80 nm with no multiple reflections. However, only slight variation of the interlayer spacing was observed for P-Al-MtXCHs, and it varied from 1.81 to 1.60 nm. We have noticed that the interlayer spacing of the PAl-MtCH precursor depended on the length of the used amine, it shifted to higher values as the length of the aliphatic chains increased.

The presence of silica was confirmed by XRF data with an increase of its content from 56% to 79%. A significant decrease in Al_2O_3 content was detected from 22 % to 5% for PAl-MtCH. In case of PAl-MtXCH materials, we noticed slight variations in SiO_2 and Al_2O_3 contents. These data confirmed that the alumina species were difficult to be exchanged with C_{12} amine when pillared clays were used.

^{27}Al MAS NMR spectrum of PAl-MtCH material exhibited different feature than Al-Mt6, with a significant increase of resonance at 52 ppm (Al^{IV}), and two resonance peaks related for Al^{VI} at 1.5 and 0 ppm. The last two peaks could be attributed to the Al^{VI} in the clay sheets and to an extra Al^{IV} existing in different environments, for example, within the intercalated silica species. Meanwhile, P-Al-Mt500CH material exhibited a similar spectrum to that reported for the starting pillared clay (described above), indicating that the stability of the alumina species between the clay sheets.

ISBN: 978-979-96595-4-5

Table 2 summarizes the textural properties of the starting pillared clays and their PCH derivatives. The PAl-MtCH material exhibited a specific surface area (SSA) of 880 m^2/g, with a total pore volume of 0.851 mL/g. This data indicated that our PAl-MtCH was mainly a mesoporous material with an average pore diameter of 3.82 nm (Table 2). The P-Al-MXCH samples exhibited SSA values lower than that of PAl-MtCH, however, higher than those of the starting pillared clays.

The total acidity of the PAl-Mt6CH (using the temperature desorption of cyclohexylamine) reached a value of 0.61 mmol/g, and higher to that of Al-Mt6 precursor and the pillared clays. Using pyridine as probe molecule, The PAl-MtXCH exhibited strong Lewis (1452 and 1617 cm^{-1}) and strong Bronsted (1540 cm^{-1} and 1640 cm^{-1}) acid sites, even at desorption temperature of 300 ^oC . While pillared clays exhibited mainly Lewis acid sites at 300 ^oC.

The hydro-isomerization reaction of heptane requires bifunctional catalysts, based on the cooperation between noble metal particles and the Bronsted acid sites. The conversion of Pt impregnated Al-Mt6 pillared clays was affected by the temperature of the catalytic reaction, and of the calcination of Al-Mt6 precursor itself. Low conversions of 2% at catalytic temperature of 250 ^oC was obtained and reached a maximum of 30 % at 350 ^oC. the calcinations of Al-Mt6 precursor at 600 ^oC and above resulted a loss of catalyst activities, up to 15 % at 350 ^oC. The selectivity to isomers and cracking products were in the range of 60% and 40 %, respectively. At catalytic temperature of 350 ^oC. The impregnated PAl-MtCH catalyst exhibited a maximum conversion of 50 % with selectivity and cracking yields of 63 and 33 %, respectively. The improvement of the conversion could be related to the nature and the strength of the acid sites in this catalyst. However, PAl-MtXCH catalysts exhibited similar conversion values compared to their starting pillared clays, calcined at temperatures higher than 400 ^oC.

The ratio of isomerization to craking (I/C) yields gave an indication on the suitability of the catalysts to the hydro- isomerization reactions. In general the I/C ratios were improved for the PAl-MtCH or PAl-MtXCH products compared to their starting pillared clays, However, the ratios were still lower than the zeolites related catalysts (in the range of 5 to 6). The stability of the catalyst was carried out at 300 ^oC, and by expanding the time on stream. The conversion and selectivity values were unchanged for a period of 12h, then a significant decrease was observed, due to the coke formation which blocked the acid sites. However, the PAl-MtCH catalyst showed a decay in catalytic activities for a period on stream of 18 h, with a mild decrease in conversion and selectivity. In case of PAl-Mt500CH, the conversion values decreased quickly for a period less than 8 h, with an improvement of the cracking products.

In conclusion, the intercalated Al_{13}-montmorillonite precursor was used to prepare pillared clays and porous clay heterostructures (PCHs). The resulting PCH from the intercalated precursor exhibited different physico-chemical properties than the pillared clays. Higher surface areas and

pore volumes were obtained. The presence of aluminum in PCH material in different environments were proofed by ^{27}Al MASNMR. Strong Lewis and Bronsted acid sites were detected at temperature of 300 ^{o}C. These sites were able to hydro-isomerize heptane molecules with a conversion of 50 % and selectivity of 63 % at 350 ^{o}C. The cracking products were about 30 %.

ISBN: 978-979-96595-4-5

Proceeding
The 2nd International Conference of the Indonesian Chemical Society 2013
October, 22-23th 2013

Characterization of Surface Area, Pore Volume and Pore Size Distribution of Activated Carbon by Physisorption Methods

Allwar[1]*, Ahmad Md. Noor[2], Mohd Asri bin Mohd Nawi[2]

[1]Chemistry Department, Faculty of Mathematics and Natural Sciences, Islamic University of Indonesia, Indonesia
[2]School of Chemistry, University Sains Malaysia, Malaysia
*allwar@uii.a.cid

Abstract

In this study, oil palm shell as solid waste from palm oil mills was used for the production of activated carbon by chemical activation using 50% $ZnCl_2$ and KOH as activating agents. Determinations of pore structures were carried out by physisorption methods using nitrogen adsorption-desorption isotherm data at 77K. Pore structures of the activated carbon were investigated and tested by variety of methods to differentiate the surface area, pore volume and pore size distribution. The difference of Langmuir shapes obtained between lower relative pressure (P/Po <0.05) and wider relative pressure (P/Po =0.05 – 0.35) have encountered a problem for characterization of pore structures. The BET, Langmuir isotherm, Dubinin-Radushkevich, Dubinin-Astakhov, t-plot and BJH methods are reliable evidences for determination of pore structures. The highest surface areas of the activated carbon are 889 and 1295 m^2g^{-1} and total pore volumes are 0.35 and 0.74 m^3g^{-1} for $ZnCl_2$ and KOH, respectively. According to the results, activated carbons prepared with KOH have wider micropore size distribution.

Keywords: nitrogen adsorption-desorption isotherm; The BET; Langmuir isotherm; Dubinin-Radushkevich; Dubinin-Astakhov; t-plot; and BJH methods.

Introduction

Well-known porous material called activated carbon has a wide range of properties and physical forms making it to be prominently used in many applications. It is extensively used in variety of industrial and environmental applications (Hu, 2001, Khalili, 2000). The important properties such as surface area, pore volume and pore size distribution including surface chemistry are among of which they are strongly associated to the adsorption capacity. Large surface area and high pore volume are widely used in chemical and gas separation, medicine and

catalyst while total surface area may supports the accessibility of active site relating to the catalytic activity (Budinova, 2006). Pore size distribution with the combinations of the micropores (pore diameter < 2nm) and mesopores (pore diameter 2 – 50 nm) are required to improve the transport process of particles or molecules inside porous networks and facilitate the adsorption of larger molecules (Lastoskie, 1993).

Due to its excellent characteristic, activated carbon has increasingly been used in numerous practical applications (Zhang, 2007). Consequently, the world consumption of activated carbon has steadily increased and also not been replaced until now, despite hard competitions from zeolite, polymer and other new-adsorbents. This can be seen from the constant increased in number of publications over the years. Recently, considerable efforts have also been increasingly directed to the comprehensive understanding of porous activated carbon

Activated carbon can be prepared from variety of byproduct solid wastes which are made of carbon-rich materials. However, a well-developed porous structure of the activated carbon depends not only on the type of byproduct solid wastes but also on the appropriate methods used to prepare it. Basically, there are two methods for preparation of activated carbon: physical and chemical activation processes. In physical process, the raw material such as wood, shell, etc. is carbonized or pyrolyzed in the absence of air and any chemicals. This is further followed by the activation process of the rudimentary solid chars in order to improve its porous structure (Guo, 2000). In chemical process, raw material is impregnated by activating agents such as phosphoric acid, potassium hydroxide, sodium carbonate, sodium hydroxide, potassium carbonate, phosphoric acid, zinc chloride, etc (Allwar, 2013). The impregnated sample is pyrolyzed under nitrogen, carbon dioxide or steam. Activation is a very important process in order to initiate a well-developed porosity by cleaning out of tars-clogging, and finally, enlarging the surface area of the activated carbon. Preparation of activated carbon with chemical activation is sometimes preferred due to some advantages in their properties which have been the focus of commercial interests (Jogtoyen, 1998).

Oil palm shell, byproduct solid waste from palm oil mills is usually burned off as solid fuel in the boiler system to produce low-energy resources and electricity, or it is discarded at open area around the mills either both practices are unfavorable to the environments (Alam, 2007). Previous studies had reported that palm shell (endocarp), a final waste from palm-oil

processing mills is a prospective precursor for the preparation of high-quality activated carbon because of its high density, relatively high carbon and low ash contents (Jaafar M., 2001, Allwar., 2008).

The purpose of this study is to prepare activated carbon and study its characterization by physisorption methods(Storck, 1998). The methods were applied using nitrogen adsorption desorption isotherm data at 77 K(Sing, 2001c). The Langmuir isotherm method was used to evaluate surface area at lower relative pressure (P/Po < 0.05), while the BET (Brunauer, Emmet and Teller) method was applied to estimate surface area at higher relative pressure (P/Po = 0.05 – 0.35) (Sing, 2001b). The Dubinin-Radushkevich (D-R) method is the most common way to evaluate the micropore volume and micropore surface area at relative pressure below 0.03(Nguyen, 2001). Micropore volume, micropore area and external surface area were estimated using t-plot method at relative pressure in the range of 0.03-0.3(Hudec, 2002). The determination of total pore volume used at single point that is the highest relative pressure (P/P_o = 0.99). The micropore diameter and mesopore diameter were calculated using Dubinin-Astakhov (D-A) and Barret-Joyner and Halenda (BJH) method, respectively (Brunauer, 1938, Lowell, 1984, Barrett, 1951, Guo, 2007).

Experimental

Sample oil palm shell was used for activated carbon production. The oil palm shell was washed with water including with hot water for removing the oil content, and dried under sunlight. The oil palm shell was crushed and sieved into particles size in the range of 0.5 – 1.5 cm.

Approximately, 250 g of each sample was impregnated with 750 ml of 50% $ZnCl_2$ and KOH solution, respectively. The mixtures were refluxed at 85^oC for 24 h. Thereafter, the mixture was filtered and the residue was washed with hot distilled water for several times until pH 6-7 by adding 5 M hydrochloride acid or 5 M sodium hydroxide. The impregnated sample then was dried in oven at 110^oC for 24 h.

Preparation of activated carbon was carried out as following procedure. The impregnated sample was carbonized in two-step process. First, the impregnated sample was loaded into stainless steel reactor and placed into the graphite furnace. Purified nitrogen gas was allowed to

flow into the reactor at a constant rate of 200 cm^3 min^{-1}. At the same time, the temperature of graphite furnace was gradually increased with a heating rate 5^oC min^{-1} to a specific temperature. The carbonization temperature was set in the range of 500 – 800^oC with a contact time 3 h. at each of process. After cooling down to room temperature, the sample was washed with hot water for several times until pH 6-7, and it then was dried in oven at 110^oC.

In the second step, similar procedure to the first step was carried out, while the purified carbon dioxide gas was allowed to flow into the reactor instead of purified nitrogen gas with the contact time of 1.5 h. The activated carbon produced was kept in tight-closed bottle for further analysis.

Proximate and ultimate analysis of activated carbon

Proximate analysis of oil palm shell was calculated using the Thermogravimetric analysis (TGA) and CNH elemental analyzer. Carbonized process was applied at temperature 30 – 900^oC, under purified nitrogen gas(Luangkiattikhun, 2008). The result was displayed in form of moisture, volatile matters and fixed carbon contents. Ultimate analysis was carried using Elemental analyzer to determine the hydrogen, nitrogen and carbon contents in the sample and activated carbon.

Result and Discussion

Thermal analysis

Table 1 shows the proximate and elemental analysis of the oil palm shell. The result shows that the carbon and oxygen proved having the major components in the oil palm shell while other elements such as hydrogen and nitrogen are presence in a relatively small quantity. The presences of high fix carbon (64.7%) and carbon (50.3%) content may be indicated that oil palm shell will be effective to be used for activated carbon precursor.

Table 1 Proximate and ultimate analysis of raw materials

Raw material	Proximate analysis				Ultimate analysis			
	Moisture (%)	Volatile matter (%)	Fix carbon (%)	Ash content (%)	Carbon (%)	Hydrogen (%)	Nitrogen (%)	Oxygen (%)
Oil palm shell	6.7	64.7	26.4	2.2	50.3	5.6	0.3	43.8

Nitrogen adsorption-desorption isotherm

Evaluation of pores structure of the activated carbon were carried out by nitrogen adsorption desorption isotherm data at 77 K. This method is one of the most important factors for estimating the type of porous materials. Series of experiment were conducted in different activation temperatures starting from 500 to 800^{o}C. Figure 1 shows the curves of nitrogen adsorption desorption isotherms at 77 K of activated carbons prepared by chemical activation using 50% $ZnCl_2$ and KOH solution. The explanation of the curves can be separated into three parts. First, the presences of open-ended shapes at temperature 400 to 600^{o}C show a poor-developed porous structure. It may be due to the insufficient heat energy to release volatile matters and finally, some of volatile matters including tar formation may block the porosity. Therefore, the absorbed nitrogen in the adsorption process cannot be completely released from the inside pores during the desorption process (Hussein, 2001). Second, most of the nitrogen adsorption-desorption isotherm shapes at higher temperatures such as at 700^{o}C show close-ended isotherms which indicate a well-porous development. The nitrogen adsorption-desorption isotherms show a steep rise in shape at lower relative pressure ($P/Po<0.05$) and a pronounced plateau at higher relative pressure ($P/Po>0.05$). This model exhibit the Type I isotherm or Langmuir isotherm associated with micropores and relatively small external surface area(Sing, 2001a). Third, for the activated carbon prepared with KOH at 700 and 800^{o}C, the curves show close-ended isotherms at low relative pressure. The isotherm shapes also show a wide knee at low relative pressure and gradually increased to unity of relative pressures indicating a well-porous development. The shapes also show typical Type I isotherms having a small hysteresis loop observed at 800^{o}C with the filling of capillary condensation. This profile indicated the presence of small external surface which is shown by hysteresis loop at near saturation relative pressure region due to the existence of wider micropores and narrower mesopores.

ISBN: 978-979-96595-4-5

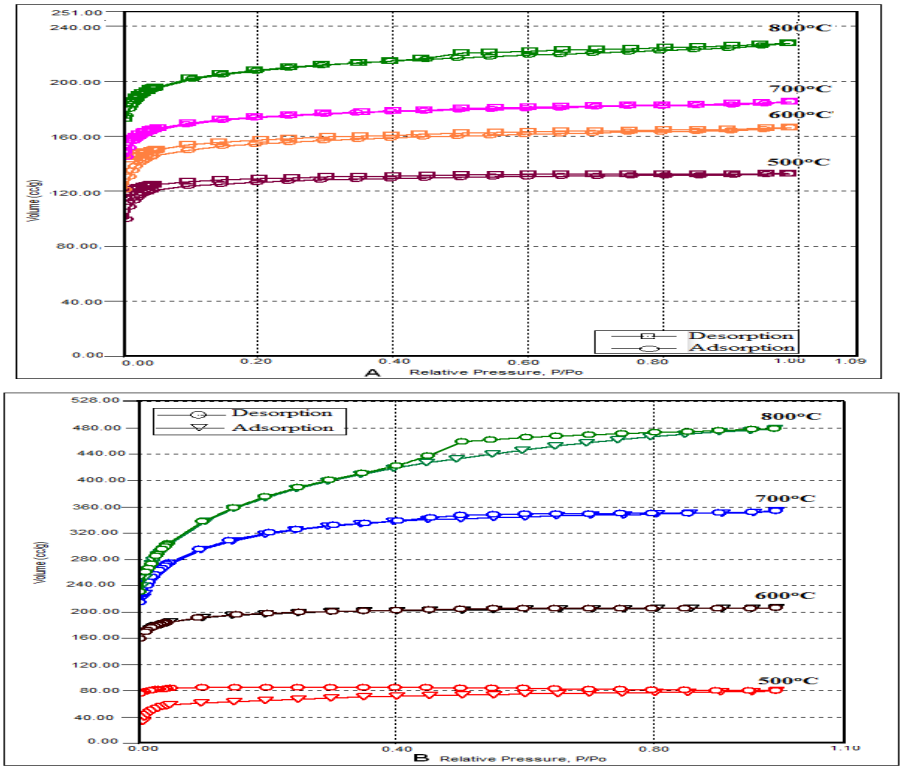

Figure 1: Nitrogen adsorption-desorption isotherms shapes of activated carbons prepared with 50% of (A) $ZnCl_2$; (B) KOH solution

Surface Area and Pore Volume

Surface area and pore volume are the most important properties that can influence the adsorption capacity of porous materials. In their applications, increasing surface area as well as pore volume is usually followed by increasing adsorption capacity. All nitrogen isotherms were observed at lower relative pressure starting from 0 to 0.05, associated with Langmuir isotherm based on the assumption that gasses form only a monolayer (**Go´mez-Serrano**, **2001)**). Consequently, the specific surface area could be better determined by the Langmuir isotherm method. Micropore volume and micropore surface area were calculated by the Dubinin-Raduskevich method based on the Type I isotherm at lower relative pressure. The values of micropores surface area are higher than the Langmuir surface area. These differences can be assumed that the Langmuir surface area were estimated from lower relative pressure (P/Po < 0.05), monolayer, while the micropores surface area can be considered as the total relative pressure consisting of monolayer and multilayer. Table 2 summarizes the textural characteristics

involving the specific surface area, micropore volume, micropore surface area and total pore volume of activated carbons.

Table 2: Textural characteristics for the yield of oil palm shell activated carbon

Type of chemical	Temperature (^oC)	Langmuir Surface area (m^2g^{-1})	Dubinin-Radushkevich		Total pore volume (cm^3g^{-1})
			Micropore volume (cm^3g^{-1})	Micropore surface area (m^2g^{-1})	
$ZnCl_2$	500	549	0.21	571	0.21
	600	664	0.25	696	0.26
	700	743	0.27	765	0.29
	800	889	0.32	906	0.35
KOH	500	297	0.11	345	0.12
	600	833	0.31	867	0.32

In contrast, the Langmuir isotherm shapes of the activated carbon prepared with KOH at 700 – 800^{o}C were observed at relative pressure in the range of 0.03 – 0.3 which have the correlation coefficient 0.99. This shape is clearly associated to the BET method for determination of surface area, meanwhile the micropore volume, external surface area and micropore area were identified with t-plot methods at the thickness in the range of 0.4- 0.6. Table 3 show the textural characteristics of activated carbon prepared with KOH at activation temperature 700 and 800^{o}C. It is clearly seen that preparation of activated carbon using KOH at higher temperature found the best result. The maximum BET surface area is 1295 m^2g^{-1} obtained at 800^{o}C. The results suggested that the activated carbon may have variety of pores consisting of wide micropores and narrow mesopores.

Table 3: Textural characteristics for the activated carbon prepared by KOH

Type of chemical	Temp (^oC)	BET surface area (m^2g^{-1})	t-plot			Total pore volume (p/po= 0.99) (cm^3g^{-1})	Mesopore Volume (cm^3g^{-1})
			Micropore volume (cm^3g^{-1})	Micropore area (m^2g^{-1})	External surface area (m^2g^{-1})		
KOH	700	1126	0.34	897	229	0.55	0.32
	800	1295	0.41	851	444	0.74	0.40

Pore Size Distribution

The measurement of pore size distribution is usually based upon the nitrogen adsorption-desorption isotherms. According to the IUPAC classification, the internal structures of porous materials can be classified into three groups: micropore (pore diameter less than 2 nm), mesopores (pore diameter in the range of 2-50 nm), and macropores (pore diameter more than 50 nm). The Dubinin-Astakhov method is widely used for determining microporous material. Previous study informed that measurement of the micropores which have lower relative pressure (P/Po< 0.05) could be carried out by the Dubinin-Astakhov (D-A) method (Gil, 2003). According to the nitrogen isotherm shapes, all activated carbons prepared with $ZnCl_2$ and KOH (exception on KOH at 700 and 800^oC) exhibit lower relative pressures. Figure 2 shows the Dubinin-Astakhov plots of pore size distributions of activated carbon. The maximum peaks of the pore diameter are located between 1.5 – 1.7 nm indication the presences of micropores or narrow micropores (pore diameter < 1.8 nm). This result is agreed with the nitrogen adsorption-desorption isotherm shapes which show Type I isotherm.

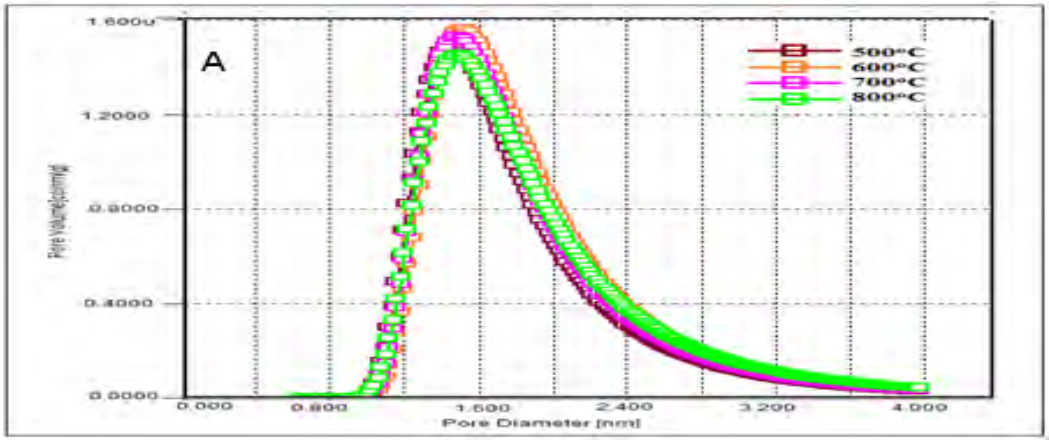

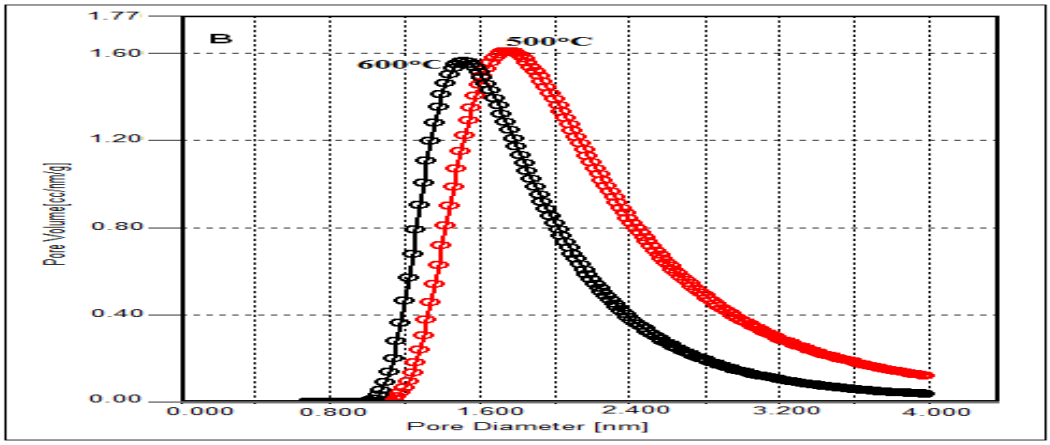

Figure 2: The Dubinin-Astakhov shapes for micropore (A) $ZnCl_2$; (B) KOH

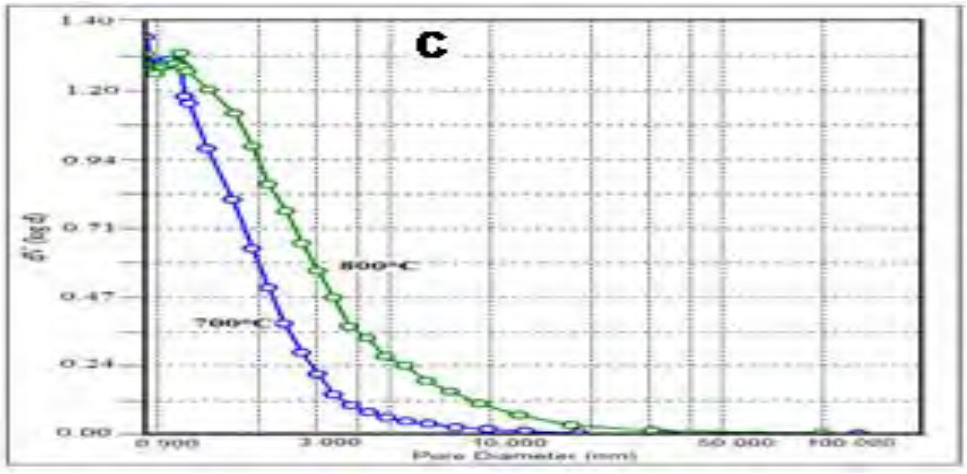

Figure 3: The BJH shape for micro- and mesopores

In contrast, the activated carbons prepared with KOH at 700 and 800°C exhibit the Type I isotherm with a small hysteresis at relative pressure higher than 0.33. It assumed that all the micropores have been filled with nitrogen as adsorbate material. Figure 3 shows the BJH shapes of the activated carbons. As seen in the figures, the shapes of pore diameters of the activated carbons are in the range from 0.9 to 50.0 nm which indicate the presence of micropores (diameter < 2 nm) and small amount of wide micropores and narrow mesopores (diameter between 1.9 – 50 nm). This result is consistent with the previous section in which the nitrogen isotherm show Type I isotherm with a small hysteresis loop.

The D-A method noticed that the quantitative micropores were estimated based on the distribution of adsorption energy (*En)* and parameter distribution (*n*) corresponding to the micropore size distribution. The values of *n* are between 1 and 4 are shown for large porous

materials. The values of n > 2 are usually for porous materials with very homogeneous micropores, while the values of n < 2 are used for heterogeneous pores with wide range micropore distributions. In this study clearly shown that the values of n are 1.9 nm which exhibit the more homogeneous pores consisting of the predominantly micropore structures. In contrast, the values of n are between 1.6 and 1.7 consisting of heterogeneous pores with wide size range of micropores. Table 4 describes the distribution of pore diameter.

Table 4: The distribution of micropore diameter of the activated carbon

Type of chemical	Temperature	BJH Average Mesopore Diameter (nm)	D-A Micropore diameter (nm)
$ZnCl_2$	500	-	1.46 (n=1.9)
	600	-	1.52 (n=1.9)
	700	-	1.48 (n=1.9)
	800	-	1.50 (n=1.8)
KOH	500	-	1.76 (n=1.7)
	600	-	1.52 (n=1.9)
	700	7.56	1.70 (n=1.7)
	800	7.87	1.76 (n=1.6)

Conclusion

The model nitrogen isotherm shapes lead the different methods that are used in the determination of pore structures. The Langmuir isotherm method, D-R and D-A methods were reliable to estimate Langmuir pore structures which have lower relative pressure, while The BET, t-plot and BJH methods were applied to estimate pore structures which have wider relative pressure. The highest surface areas of the activated carbon are 889 and 1295 m^2g^{-1} and total pore volumes are 0.35 and 0.74 m^3g^{-1} for $ZnCl_2$ and KOH, respectively. The activated carbon prepared with $ZnCl_2$ clearly show micropore size distribution, while the activated carbon prepared with KOH exhibit heterogeneous-pore size distribution: wider micropores and narrow mesopores

Acknowledgment

The authors acknowledge the scientific fund of University Islam Indonesia, Yogyakarta, Indonesia and Universiti Sains Malaysia, Malaysia for financial support.

References

ALAM, M. Z., MUYIBI, S.A., MANSOR,M.F., WAHID, R. (2007) Activated carbon deriver from oil palm empty-fruit bunches: Application to environmental problem. *Journal of Environmental Sciences,*.

ALLWAR (2013) Porous Structures of Activated Carbons Derived from Oil Palm Empty Fruit Bunch by Phosphoric Acid Activation under Nitrogen and Carbon Dioxide. *International Journal of Research in Chemistry and Environment,* 3**,** 62-68.

ALLWAR., A., M. N., ASRI, M. (2008) Textural Characteristics of Activated Carbons Prepared from Oil Palm Shells Activated with $ZnCl_2$ and Pyrolysis Under Nitrogen and Carbon Dioxide. *Journal of Physical Science,* 19**,** 93-104.

BARRETT, E. P., JOYNER, L.G., HALENDA, P.P. (1951) The determination of pore volumes and area distributions in porous substances. *J. Am. Chem. Soc,* 73**,** 373-380.

BRUNAUER, S., EMMET, P.H., TELLER, F. (1938) Surface area mesurements of activated carbons, silica gel and adsorbents. *Am. Chem. Soc,* 60.

BUDINOVA, T., EKINCI, E., YARDIM, F., GRIMM, A., BJÖRNBOM, E., MINKOVA, V. AND GORANOVA, M., . (2006) Characterization and application of activated carbon produced by H3PO4 and water vapor activation *Fuel Processing Technology,* 87.

GIL, A., AND GANDIA, L.M. (2003) Microstructure and quantitative estimation of the micropore-size distribution of an alumina-pillared clay from nitrogen adsorption at 77 K and carbon dioxide adsorption at 273 K. *Chemical Engineering Science,* 58**,** 3059 - 3075.

GO´MEZ-SERRANO, V., GONZA´LEZ-GARC´ıA, C.M. AND GONZ´ALEZ-MART´ıN, M.L. (2001)) **Nitrogen adsorption isotherms on carbonaceous materials. Comparison of BET and Langmuir surface areas.** ***Powder Technology*****, 116, 103-108**.

GUO, J., AND LUA, A.C (2000) Preparation of activated carbons from oil palm stone char by microwave induced carbon dioxide activation. *Carbon,* 38**,** 1985-1993.

GUO, Y., ROCKSTRAW, D. A. (2007) Activated carbon prepared from rice hull by one-step phosphoric acid activation. *Microporous and Mesoporous Materials,* 100**,** 12-19.

HU, Z., SRINIVASAN, M.P. (2001) Mesoporous high-surface-are activated carbon. *Microporous and Mesoporous Materials,* 43**,** 267-275.

HUDEC, P., SMIESKOVA, A., ZIDEK, Z., SCHNEIDER, P., SOLCOVA, O. (2002) Determination of Microporous Structure of Zeolites by t-Plot Method - State-of-the-Art. *Studies in Surface Science and Catalyst,* 142**,** 1587-1594.

HUSSEIN, M. Z., ABDUL RAHMAN, M. B., YAHYA, A., TAUFIQ-YAP, Y. H., AHMAD, N. (2001) Oil palm trunk as a raw material for activated carbon production. *Journal of Porous Material,* 8**,** 327-334.

JAAFAR M., S. J. (2001) The future of palm oil in the new millennium in Malaysia. *Burotrop Bulletin,* 16**,** 123-131.

JOGTOYEN, M., DERBYSHIRE, F. (1998) Activated carbon from yellow poplar and white oak by H3PO4 activation. *Carbon,* 36**,** 1085-1097.

KHALILI, N. R., CAMPBELLA, M., SANDI, G., GOLAS, J. (2000) Production of micro- and mesoporous activated carbon from paper mill sludge I. Effect of zinc chloride activation. *Carbon,* 38**,** 1905-1915.

LASTOSKIE, C., GUBBINS, K.E. AND QUIRK. . J. PHYS. CHEM., 97, 4786-4796 (1993) Pore size distribution analysis of microporous carbons: a density Functional theory approach. *J. Phys. Chem.,* 97.

LOWELL, S., SHIELDS, J.E. (1984) Powder Surface Area and Porosity. second ed ed. New York., John Wiley.

LUANGKIATTIKHUN, P., . TANGSATHITKULCHAI, C., TANGSATHITKULCHAI, M. (2008) Non-isothermal thermogravimetric analysis of oil-palm solid wastes. *Bioresource Technology,* 99**,** 986-998.

NGUYEN, C., DO, D. D. (2001) The Dubinin–Radushkevich equation and the underlying microscopic adsorption description. *Carbon,* 39**,** 1327-1336.

SING, K. (2001a) Review: The use of nitrogen adsorption for the characterisation of porous materials. *Colloids and Surfaces A: Physicochemical and Engineering Aspects,* 187-188**,** 3-9.

SING, K. (2001b) The use of nitrogen adsorption for the characterisation of porous materials. *Colloids and Surfaces A: Physicochemicala nd Engineering Aspects,* 187-188**,** 3-9.

SING, K. S. W. (2001c) Review. The use of nitrogen adsorption for the characterization of porous materials. *Colloids and Surfaces A: Physicochemical and Engineering Aspects,* 187-188**,,** 3-9.

STORCK, S., BRETINGER, H. AND MAIER, W. F (1998) Characterization of micro- and mesoporous solids by physisorption methods and pore-size analysis. *Applied Catalysis A: General,* 174**,** 137-146.

ZHANG, Y., ZHENG, J., QU, X., CHEN, H. (2007) Effect of granular activated carbon on degradation of methyl orange when applied in combination with high-voltage pulse discharge. *Journal of Colloid and Interface Science,* 316**,** 523-530.

Proceeding
The 2nd International Conference of the Indonesian Chemical Society 2013
October, 22-23th 2013

Synthesis and electrochemical characterization of Nickel-Cobalt Porous Electrode

Riyanto

Chemistry Study Program, Faculty of Mathematics and Natural Science,
Universitas Islam Indonesia, Jl. Kaliurang KM 14.5 Yogyakarta 55584
e-mail: riyanto@uii.ac.id

Abstract

Electrochemical activity of cobalt and nickel materials strongly depends on their morphology, surface area, structure and composition. Synthesis and electrochemical characterization of Nickel-Cobalt Porous Electrode in alkaline solution has been done. Ni-Co porous electrode were prepared using mechanical alloying technique (MAT) with polyvinyl chloride (PVC) and tetrahydrofuran (THF) used as the binding and solvent. The total weighed of the pellet obtained is approximately 1.5 g. This material is then heated in a furnace with a various temperature of 100, 300, 600 and 900^{o}C. Universal Pulsa Dynamic EIS, Voltammetry, Voltalab potentiostat (Model PGZ 402) was used for electrochemical characterization measurement. Cyclic voltammetry experiments were performed in three electrodes system using Ni-Co porous electrode, SCE and platinum wire, which acts as the working (anode), reference and counter electrode respectively. The SEM micrograph of a Ni-Co porous electrode shows the rough, irregular and porous characteristic of the surface of the electrodes. Base on cyclic voltammetry shows cobalt and nickel porous electrode indicated that the good stability and electrochemical catalytic activity.

Keywrods: Synthesis, Ni-Co porous electrode, Electrochemical Characterization

Introduction

Electrocatalytic activity of these materials strongly depends on their morphology, surface area and structure, which in turn depend on the preparation methods. Powders of nickel and copper are widely used in numerous applications because they possess good catalytic, electronic and magnetic properties (Bonet et al. 2003). Cobalt and nickel, being transition elements, with their electronic layer *d* incomplete, have shown good electrocatalytic properties (Contreras et al. 2007). Nickel and copper powders are extensively used as electrode material in solid oxide fuel cells. When a metal is associated with another metal in bimetallic or alloy form, the properties of the resulting material can be enhanced with respect to those of the pure metals. This is the case for Ni-based bimetallic particles containing copper, which exhibit better catalytic activity and selectivity than monometallic nickel (Songping et al. 2007).One of the techniques of making the porous electrode is by incorporating polymer material like polyvinyl chloride (PVC) with the powder of respected metals (Pereira et al. 2004).

Pore size, pore structure, permeability, and surface area are some of the important characteristics that need to be measured for designing efficient electrodes and separators as well as evaluating their performance. Porous electrodes are found throughout electrochemistry, because of enhanced charge storage capacities and/or enhanced electrochemical Faradaic transfer rates. The advantages of porous electrodes is the large surface area means that a large area for double layer formation. Electrochemical capacitors take advantage of this concept (Castro et al. 2004).

It was found that the electrical and mechanical properties in porous electrodes dramatically change depending on the pore size and the dielectric constant of the medium. For a low dielectric constant of the medium, the capacitance of porous electrodes tends to increase as the pore size decreases and the pressure in the porous electrodes is positive or negative depending on the pore size. PVC resin can be used for Ni-PVC composite electrode as a good catalyst in concentrated KOH solutions (Gonzales et al. 1997).

In this paper we present results on the synthesis of Ni–Co bimetallic porous electrode (50:50 weight ratios) using powder of nickel and copper, and tetrahydrofuran (THF) as solvent and polyvinyl chloride (PVC) as binding agent. To improve the properties of Ni-Co-PVC, several methods have been proposed for the preparation of Ni-Co porous electrode with heated at 100, 300, 600 and 900^{o}C. Ni–Co porous electrode was characterized by FTIR and scanning electron microscopy coupled with energy dispersion X-ray for microanalysis. Electrochemistry investigation of Ni–Co porous electrode using cyclic voltammetry (CV), linear voltammograms and Tafel plot. Cyclic voltammetry methods are employed to characterize the electrochemical properties of this electrode material in a N_2-saturated alkaline solution.

Experimental

Synthesis

Nickel-cobalt-polyvinyl chloride electrode was prepared by mixing a weighed portion of Co powder (< 2 micron in size and 99.9% purity, Systerm), Ni powder (< 2 micron in size and 99.9% purity, Aldrich Chemical Company) and PVC in 4 ml tetrahydrofuran (THF) solvent and swirled flatly to homogeneous followed by drying in an oven at 100^0 C for 3 hours. The mixture was placed in 1 cm diameter stainless steel mould and pressed at10 ton/cm^2. A typical pellet contained approximately amount of Co (47.5%) and Ni (47.5%) powder, and

approximately 5% of PVC polymer. The total weighed of pellet obtained is approximately 1.5 g. This material heated at various temperatures of 100, 300, 600 and 900^{o}C using furnace.

Characterization

The surface characterization of the electrode using SEM and EDS was performed on the JSM 5400 microscope equipped with a microprobe Voyager Noran system. IR spectra were obtained using a Nicolet Avatar 370Dtgs spectroscopy; the samples were mixed with KBr and pressed as pellets.

The electrochemical characterization of materials was carried out by cyclic and linear voltammetry techniques. Universal Pulsa Dynamic EIS, Voltammetry, Voltalab potentiostat (Model PGZ 402) was used for electrochemical behavior measurements; data acquisition was accomplished using the Voltamaster 4 software. Cyclic voltammetry experiments were performed in a three electrodes system using Ni-Co-PVC as a working electrode (anode), an Ag/AgCl (saturated KCl) or SCE as reference electrode and platinum wire as the counter electrode. All potentials given are with respect to the SCE reference electrode. The electrochemical studies by cyclic voltammetry (CV) and oxidation of ethanol by potentiostatic (chronocoulometry) method were performed in 25 mL capacity glass electrochemical cell.

Result and Discussion

Fig. 1A-1D showed the morphological study of Ni-Co porous electrode with various temperatures at cross section by SEM and EDX. Fig. 1A and 1B showed the morphological at cross section $Ni_{47.5}Co_{47.5}$-PVC_5 material with temperature 100 and 300 ^{o}C. Fig. 1A and 1B showed the PVC as a binder metal Ni and Co, this result is supported by the peak chloride atom at EDX spectra. The effect of heating at temperatures 600 and 900 ^{o}C resulted in the loss of PVC from this material (Fig 1C and 1D).

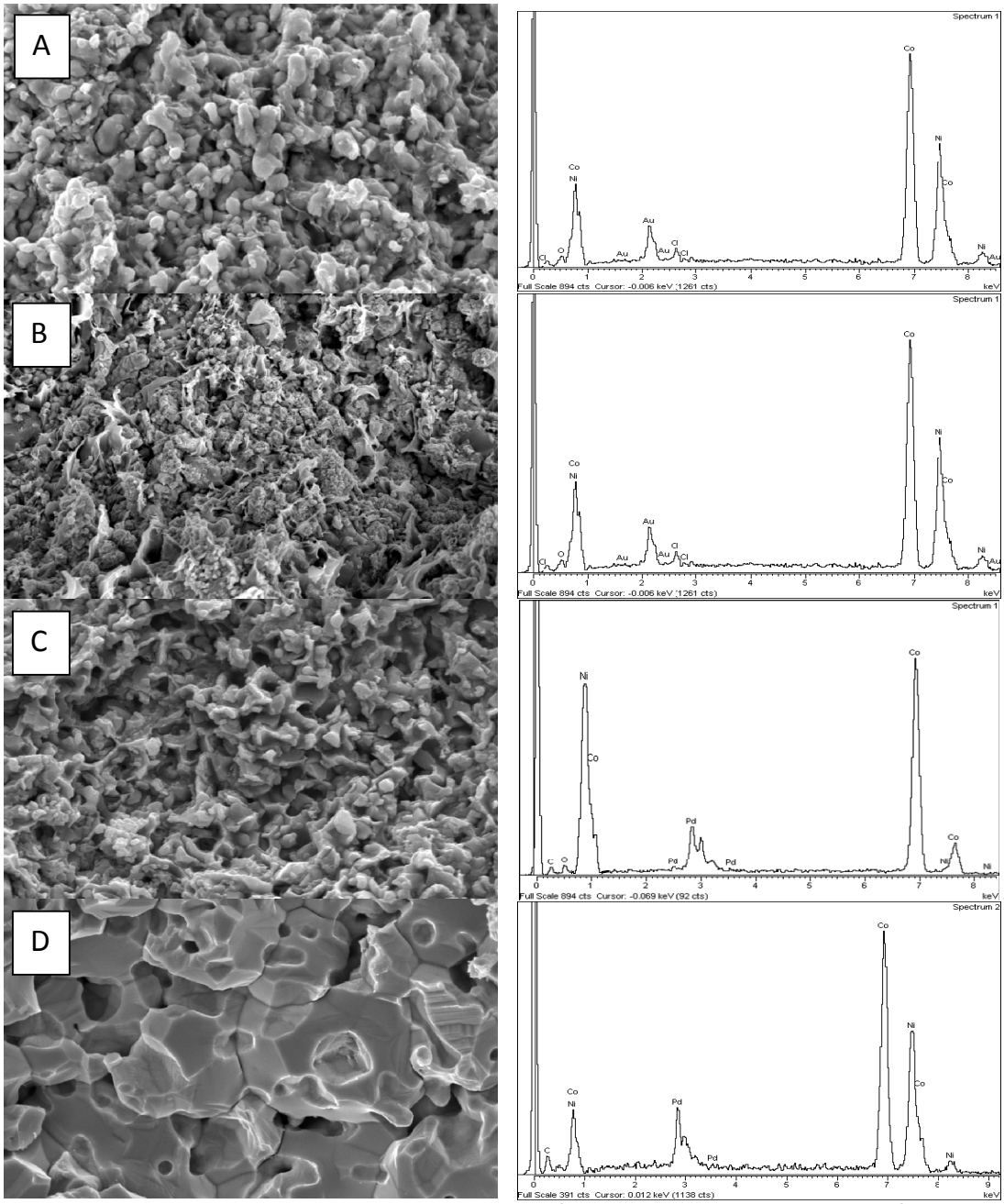

Fig. 1. SEM photographs and EDX spectrum of $Ni_{47.5}Co_{47.5}$-PVC_5 electrode after press at 10 tan/cm^2 and heated with various temperatures of (A) 100 (B) 300 (C) 600 and (D) 900^oC

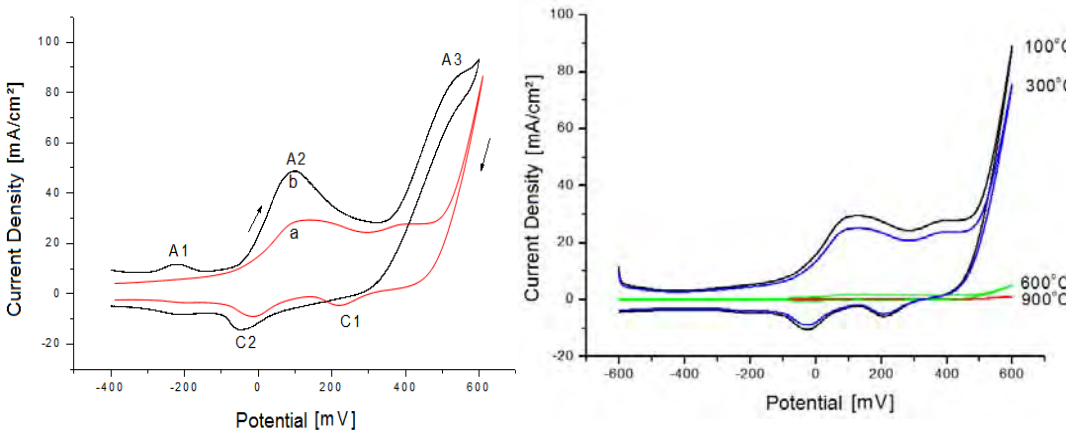

Fig 2. Cyclic voltammogram of $Ni_{47.5}Co_{47.5}$-PVC_5 fres electrode (a) 1.0 M KOH dan (b) 0.25 M etanol + 1.0 M KOH. Scan rate 10 mVs^{-1} (A) and (B) Cyclic voltammogram of $Ni_{47.5}Co_{47.5}$-PVC_5 at virious temperature in 1.0 M KOH scan rate 50 mVs^{-1}

Fig 2A and 2B shown cyclic voltammogram of $Ni_{47.5}Co_{47.5}$-PVC_5 fres electrode (a) 1.0 M KOH dan (b) 0.25 M etanol + 1.0 M KOH. Scan rate 10 mVs^{-1} (A) and (B) Cyclic voltammogram of $Ni_{47.5}Co_{47.5}$-PVC_5 at virious temperature in 1.0 M KOH scan rate 50 mVs^{-1}. C1 and C1' peaks at Fig. 2A is a reduction peaks for Ni (III) in the form of NiOOH to Ni (II) which is in the form of $Ni(OH)_2$. This process is similar to the C1 peak at Fig.2A. According to Hahn et al. (1986 and 1987) C1 peak at Fig. 2A, represent peaks for the formation of β-NiOOH**,** while peak C2 at Fig. 2A which do not appeared in Fig. 5A is explained by the existence of crystallographic form γ-NiOOH. According to Casella et al. (1999), α-form is known to be unstable in alkaline solution and slowly converted and irreversible to the β-form, while on prolonged charging; β-NiOOH converts to the γ-oxyhydroxide form. C1 peak at Fig. 2A is a reduction peak for Ni (III) (in the form of NiOOH) to Ni (II) which is in the form of $Ni(OH)_2$ and C2 peak at Fig. 2A is a reduction peak for Co (III) in the form of CoOOH to Co (II) which is in the form of $Co(OH)_2$. The effects of heating in high temperatures, current density results in lower because many holes formed (Fig 1D).

ISBN: 978-979-96595-4-5

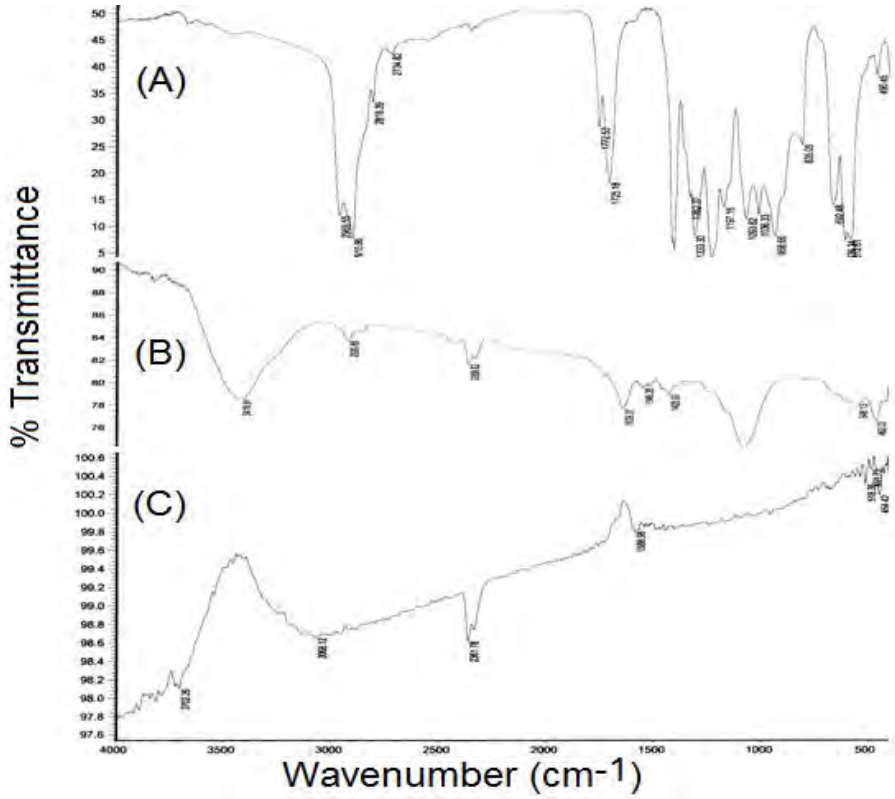

Fig.3. FTIR spectra of (A) PVC and THF (B) $Ni_{47.5}Co_{47.5}$-PVC_5 after heated at temperature 100 and 300 and (C) 600 and 900^oC

Fig.3 shows the FTIR spectra of the investigated the effect of heated at $Ni_{47.5}Co_{47.5}$-PVC_5 material after heated at temperature 100, 300, 600 and 900^oC. Fig. 3C has shown the FTIR spectra loss peak from PVC compound. The peaks at around 3450 cm-1 correspond to molecular hydrogen bonded with Ni and Co metals. Comparing the infrared spectra of Fig. 3A, 3B, and 3C, it is clear that the effect heated at high temperature cause of PVC loss from material. Fig.3A. peak at 1425 cm^{-1}, 959 cm^{-1} and 610 cm^{-1} are peaks originating from the PVC. The infrared spectra of PVC consist of C-Cl stretching vibration near 610 cm^{-1}.

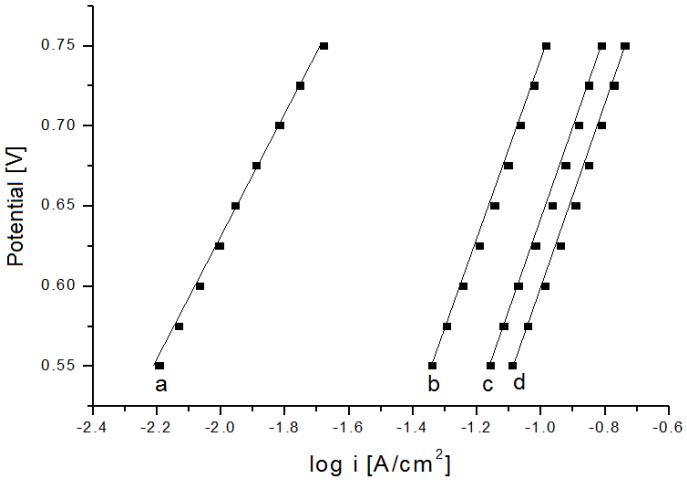

Fig. 4. Tafel plot for $Ni_{47.5}Co_{47.5}$-PVC_5 electrode in 0.25 M ethanol + 1.0 M KOH with scan rate 1 mVs^{-1} after heated at temperature (A) 900 (B) 600 (C) 300 and (D) 100^oC.

The Tafel equation is an equation in electrochemical kinetics relating the rate of an electrochemical reaction to the overpotential. As shown in Fig. 4, the catalytic oxidation $Ni_{47.5}Co_{47.5}$-PVC_5 electrode in 0.25 M ethanol + 1.0 M KOH with scan rate 1 mVs^{-1} after heated at temperature 900, 600, 300 and 100^oC. Fig. 4 compares the Tafel plots of the electrodes of $Ni_{47.5}Co_{47.5}$-PVC_5 with various temperatures. The Tafel plots were recorded from 550 to 750 mV with a scan rate of 1 mVs-1. The $Ni_{47.5}Co_{47.5}$-PVC_5 electrode heated at 100 and 300^oC has higher catalytic activity for ethanol in 0.1 M KOH electro-oxidation, which is well consistent with the above analysis.

Conclusions

A composite material, $Ni_{47.5}Co_{47.5}$-PVC_5, is synthesized using the mechanical alloy method with the purpose to develop electrode materials for electro-synthesis. Physical characterization using XRD, EDX, and SEM show that $Ni_{47.5}Co_{47.5}$-PVC_5 possesses an amorphous structure. The results demonstrate that this material good electrochemical oxidation activity ethanol in 0.1 M KOH solution. The effects of heated at high temperature cause this $Ni_{47.5}Co_{47.5}$-PVC_5 material change to alloy with high porous. The $Ni_{47.5}Co_{47.5}$-PVC_5 has properties very low electrochemical oxidation activity ethanol in 0.1 M KOH solution.

Acknowledgements

Sincere thanks are due to the Universitas Islam Indonesia and University Kebangsaan Malaysia (UKM) for their financial support and instrumentation analysis.

References

Bonet, F., Grugeon, S., Dupont, L. Urbina, R.H., Guery, C. & Tarascon, J.M. 2003. Synthesis and characterization of bimetallic Ni–Cu particles. *Journal of Solid State Chemistry* 172: 111–115.

Castro E.B., Real S.G. and Pinheiro, D.L.F. 2004. Electrochemical characterization of porous nickel-cobalt oxide electrodes, *International Journal of Hydrogen Energy*, 29 (3): 255–261.

Casella, I.G., Guascito, M.R. & Sannazzaro, M.G. 1999. Voltammetric and XPS investigations of nickel hydroxide electrochemically dispersed on gold surface electrodes. *J. Electroanal. Chem*. 462: 202-210.

Contreras, M.A.G., Valverde, S.M.F. & Garcia, J.R.V. 2007. Oxygen reduction reaction on cobalt-nickel alloys prepared by mechanical alloying. *Journal of Alloys and Compounds* 434-435: 522-524.

Gonzalez, M., Elizalde, M.P., Banos, L., Poillerat, G. & Davila, M.M. 1999. Surface characterization of $LaNiO_3$/Ni-PVC composite. *Electrochim. Acta* 45: 741-750.

Hahn, F., Beden, B., Croissant, M.J. & Lamy, C. 1986. In situ UV visible reflectance spectroscopic investigation of the nickel electrode-alkaline solution interface. *Electrochim. Acta* 31: 335-342.

Hahn, F., Beden, B., Croissant, M.J. & Lamy, C. 1987. In situ investigation of the behaviour of a nickel electrode-alkaline solution by UV visible and IR reflectance spectroscopic. *Electrochim Acta* 32: 1631-1636.

Pereira, M.G., Jimenez, M.D., Elizalde, M.P., Robledo, A.M. & Vante, N.A. 2004. Study of the electrooxidation of ethanol on hydrophobic electrodes by DEMS and HPLC. *Electrochim. Acta* 49: 3917-3925.

Songping, W., Li, J., Jing, N., Zhenou, Z. & Song, L. 2007. Preparation of ultra fine copper-nickel bimetallic powders for conductive thick film. *Intermetallics* 15: 1316-1321.